INVESTIGATING HOUSING PRICES IN INDIA THROUGH LINKAGES, SPILLOVERS, WAVELET COHERENCE, AND CONNECTEDNESS WITH MACROECONOMIC VARIABLES

Sponsored by: National Housing Bank, New Delhi, India

Submitted by:

Professor Rudra P. Pradhan, Indian Institute of Technology, Kharagpur, India (Principal Coordinator)

Authors/ Team Members:

- **Professor Rudra P. Pradhan, Indian Institute of Technology, Kharagpur, India (Principal Coordinator)**
- **Dr. SMRK Samarakoon, Indian Institute of Technology, Kharagpur, India and Wayamba University of Sri Lanka, Kuliyapitiya, Sri Lanka**
- **Dr. Gayan Chathuranga, Wayamba University of Sri Lanka, Kuliyapitiya, Sri Lanka**
- **Mr. Supun Kumara, Department of Business Economics, Faculty of Management Studies and Commerce, University of Sri Jayewardenepura, Sri Lanka**

Acknowledgement

We gratefully acknowledge the financial and administrative support of the National Housing Bank (NHB) for the project titled "Investigating Housing Prices in India through Linkages, Spillovers, Wavelet Coherence, and Connectedness with Macroeconomic Variables." We are especially thankful to National Housing Bank (NHB) for their timely guidance, the commencement clearance, and the mid-term review arrangements.

We also thank Indian Institute of Technology Kharagpur for infrastructure and academic support, and our collaborators, research associates and student assistants for their diligent contributions. Any remaining errors are our own, and the opinions expressed here do not necessarily represent those of NHB.

Abstract

This study examines housing prices in India using daily return and volatility linkages for a market proxy—the Real Estate Sector Index (RESI)—and quarterly nonlinear dynamics for the Housing Price Index (HPI). Daily connectedness is estimated with a time-varying parameter vector autoregression (TVP-VAR) and a dynamic conditional correlation GARCH (DCC-GARCH); time–frequency co-movement is assessed with wavelet coherence; quarterly relations are evaluated with a nonlinear autoregressive distributed lag (NARDL). TVP-VAR results show the NIFTY50 equity index as the main transmitter of return spillovers to RESI and the U.S. dollar/Indian rupee exchange rate (USD/INR), while the Consumer Price Index (CPI) and the 91-day Treasury bill rate transmit little at high frequency. DCC-GARCH indicates that NIFTY50 and RESI transmit volatility; RESI and USD/INR are net receivers; CPI and the Treasury bill rate have near-unity own-variance shares. Wavelet coherence shows horizon-dependent relations, with interest-rate and exchange-rate effects concentrated at lower frequencies. In quarterly NARDL estimates for 2012Q1–2025Q1, increases in the 91-day Treasury bill rate have a positive short-run association with HPI, while contemporaneous real gross domestic product (log), CPI, and Economic Policy Uncertainty (EPU) are not statistically different from zero; the bounds test indicates no cointegration. Findings imply a separation between high-frequency equity-driven transmission to housing valuations and lower-frequency policy channels affecting quarterly prices.

Keywords: housing prices; macroeconomic variables; connectedness; TVP VAR, DCC-GARCH; wavelet coherence; NARDL; India.

1. Introduction

Housing prices interact with macroeconomic conditions through credit, investment, and wealth channels. These interactions affect monetary transmission, household balance sheets, and financial stability. India has experienced structural changes in housing demand, financial deepening, and regulation over the past two decades. Yet the frequency-specific and time-varying relationships between Indian housing prices and macroeconomic variables remain insufficiently documented.

International research links housing prices to output, interest rates, inflation, employment, money, exchange rates, and financial markets. Studies using country-specific VAR and error-correction frameworks report responses of housing prices to monetary and real shocks and quantify variance contributions from macroeconomic drivers (Apergis & Rezitis, 2003; Baffoe-Bonnie, 1998). Evidence from multi-country settings shows co-movement between real housing prices and global macro-financial factors, with spillovers that extend beyond domestic conditions (Beltratti & Morana, 2010; Adams & Füss, 2010). Within-country analyses also identify heterogeneity by region and city tier and highlight roles for money growth, mortgage rates, construction costs, and demographics (Zhang, Li, Hui, & Li, 2016; Duan, Tian, Yang, & Zhou, 2020; Sivitanides, 2018). Other contributions emphasize regime dependence in housing–macro linkages using Markov-switching models and document distinct “boom,” “tranquil,” and “downturn” states (Nneji, Brooks, & Ward, 2013), while forecasting studies underscore the predictive content of policy and price variables for housing returns and regime probabilities (Chen, Cheng, & Mao, 2013). OECD evidence further indicates error-correction toward long-run relations among house prices, income, and interest rates and changing cross-country synchronization over time (Kishor & Marfatia,

2017). At the same time, city- and micro-level hedonic analyses reveal spatial variation in attributes and access to amenities, which complements the macro focus (Duan et al., 2020).

Recent work incorporates uncertainty and stress indicators into housing analyses. Wavelet and volatility-based approaches detect time- and frequency-dependent co-movements between housing markets and policy or financial uncertainty and quantify spillovers across assets and regions (Kirikkaleli et al., 2021; Paul et al., 2024). These methods are well suited to environments with evolving policy regimes and market structures.

Despite this body of evidence, two gaps remain for India. First, most Indian studies rely on static or single-frequency methods and do not integrate time variation with frequency decomposition. Second, the joint role of equity market conditions, exchange rates, inflation, interest rates, and economic policy uncertainty (EPU) in shaping Indian housing prices has not been examined within a unified spillover and connectedness framework that links short-horizon financial dynamics to lower-frequency macro adjustments. Addressing these gaps is relevant for policy design, risk assessment, and portfolio allocation in a setting with evolving regulation, urbanization, and capital market development.

This paper investigates dynamic linkages and spillovers between Indian housing prices and key macro-financial variables using complementary time- and frequency-domain tools. The analysis proceeds on two data tracks. For higher-frequency behavior, we use daily series for a real estate equity index as a market-based proxy for housing sector valuations, along with stock market, exchange rate, inflation proxy, interest-rate proxy, and EPU. For lower-frequency adjustments, we use quarterly housing price index (HPI), GDP, inflation, interest rates, and EPU. This design

permits joint assessment of short-horizon co-movements and long-run relations and enables cross-validation of results across frequencies.

Methodologically, we combine wavelet coherence, time-varying connectedness, and conditional correlation with an asymmetric long-run model. Wavelet coherence decomposes co-movements by scale and time and identifies lead–lag patterns between housing prices and macro-financial drivers (Torrence & Compo, 1998). A time-varying parameter VAR with forecast error variance decomposition provides connectedness measures and spillover indices that evolve through time, aligning with the approach popularized in financial contagion studies (Diebold & Yilmaz, 2012). A DCC-GARCH specification captures shifts in conditional correlations and volatility transmission between housing and macro-financial series (Engle, 2002). For quarterly data, a nonlinear ARDL (NARDL) model captures asymmetric short-run and long-run effects consistent with threshold-like responses of housing prices to positive and negative movements in macro variables, extending ARDL applications to the Indian housing context (Parrikar, 2020).

The study addresses three questions. First, what are the dynamic linkages and spillover effects between Indian housing prices and macro-financial variables across horizons? Second, how do short-run and long-run relationships evolve through time and across policy episodes? Third, to what extent does EPU influence housing price dynamics and stability?

We report three contributions. First, we integrate wavelet coherence with time-varying connectedness and DCC-GARCH to map Indian housing–macro interactions across frequency, time, and volatility channels in a single study. Second, we link daily market-based indicators with quarterly macro aggregates to connect high-frequency risk transmission to lower-frequency adjustments in fundamentals. Third, we quantify the role of EPU in Indian housing dynamics

within both the spillover network and the long-run asymmetric framework, extending uncertainty-housing evidence from other jurisdictions to India.

The empirical design builds on established findings while adapting them to India. VAR and ECVAR studies document macro shocks that propagate into housing prices and sales (Apergis & Rezitis, 2003; Baffoe-Bonnie, 1998). Panel cointegration results suggest long-run elasticities with respect to activity, construction costs, and long-term rates and slow adjustment to equilibrium (Adams & Füss, 2010). Global factor and international synchronization studies point to cross-border linkages in housing cycles and macro drivers (Beltratti & Morana, 2010; Kishor & Marfatia, 2017). City-level analyses show that monetary variables and mortgage rates act through credit conditions, while local attributes generate spatial heterogeneity (Zhang, Hua, & Zhao, 2012; Duan et al., 2020). Wavelet, connectedness, and volatility frameworks capture the multi-scale and evolving character of these links and have been applied to housing and uncertainty in other settings (Torrence & Compo, 1998; Diebold & Yilmaz, 2012; Engle, 2002; Kirikkaleli et al., 2021; Paul et al., 2024). By importing these tools to the Indian context and using both daily and quarterly frequencies, the present study provides evidence on the scale at which co-movements and spillovers are strongest, the direction of net transmissions through time, and the asymmetry of long-run responses.

The remainder of the paper is organized as follows. Section 2 reviews the literature on housing–macro linkages, spillovers, and frequency-domain analysis with a focus on evidence relevant to emerging markets. Section 3 describes data sources, variable construction, and frequency alignment and the econometric framework, including wavelet coherence, TVP-VAR

connectedness, DCC-GARCH, and NARDL. Section 4 presents results and Section 6 concludes with implications for policy and investment.

2. Literature Review

The existing literature links housing prices to macroeconomic activity, prices, interest rates, credit and money, exchange rates, and demographic or spatial factors through cointegration, VAR/ECVAR, and VECM frameworks; documents regime dependence and time variation with Markov switching and Bayesian time-varying VARs; measures volatility clustering and asymmetric responses with EGARCH and DCC-type specifications; and analyzes multi-scale co-movements using wavelet methods. Evidence spans advanced and emerging economies and city-level settings, with studies reporting heterogeneity across tiers and regions and noting the role of policy regimes and financial conditions. This body of work motivates an integrated empirical strategy that connects short-horizon risk transmission to lower-frequency adjustments and accommodates evolving dependence, spillovers, and spatial features.

Research links housing prices to macroeconomic activity, prices, and interest rates in both national and international settings. Panel evidence across 15 countries reports cointegration between house prices, economic activity, construction costs, and long-term rates, with slow adjustment to equilibrium (Adams & Füss, 2010). Vector autoregression analyses for OECD economies show that interest-rate shocks reduce real house prices and that house price innovations feedback to output, prices, and policy rates (Demary, 2010). For the G7, co-movement between real housing prices and global macro-financial factors is documented, with spillovers traced to common supply-side shocks and international business-cycle linkages (Beltratti & Morana, 2010). Error-correction behavior in the long run between house prices, income, and interest rates is reported for OECD

countries, with time variation in cross-country synchronization (Kishor & Marfatia, 2017). Country and city evidence further ties prices to income, supply, unemployment, and GDP through cointegration and VECM frameworks (Baffoe-Bonnie, 1998; Al-Masum & Lee, 2019). Studies of Turkey and China identify roles for monetary aggregates, mortgage credit, and land supply in shaping housing activity and prices (Sari, Ewing, & Aydin, 2014; Li, Razali, Fereidouni, & Adnan, 2018). U.S. evidence shows that expected inflation and unemployment help explain local price changes and forecastability at the city level (Clapp & Giaccotto, 1994).

Monetary conditions and mortgage rates are central channels. For Greece, an ECVAR with impulse responses and variance decompositions shows responses of new-house prices to loan rates, inflation, and employment (Apergis & Rezitis, 2003). For Beijing, VAR results associate higher money supply and lower mortgage rates with higher prices over longer horizons, while hedonic attributes vary in space (Duan, Tian, Yang, & Zhou, 2021). A nonlinear NARMAX–VECM for China highlights mortgage rates, producer prices, broad money, and the real effective exchange rate as key drivers, while income is not independently decisive (Zhang, Hua, & Zhao, 2012). A Markov-switching study for the United States shows regime-dependent sensitivities and points to interest-rate spreads as a policy lever for regime transitions (Nneji, Brooks, & Ward, 2013). Cross-country work on EU markets examines similarities in demand- and supply-side responses and discusses implications of monetary union for market integration (Kasparova & White, 2010). A structural macro model with segmented financial markets shows that mortgage-rate reductions raise prices and that loan-to-value relaxations have ambiguous effects, accounting for a material share of the 2000s U.S. price increase (Garriga, Manuelli, & Peralta-Alva, 2019). Very long U.S./U.K. samples under Bayesian time-varying VARs attribute U.S. house price movements

mainly to technology shocks and U.K. movements to monetary policy shocks (Plakandaras, Gupta, Katrakilidis, & Wohar, 2020).

Dynamic causality and instability are recurrent themes. Granger-causality tests for Victoria show lagged interrelations between macro variables and prices that shift across subperiods, complicating prediction (Luo, Liu, & Picken, 2007). Time-varying connectedness and conditional correlation frameworks motivate measuring spillovers and evolving dependence; these are operationalized in practice with forecast-error-variance decompositions from time-varying parameter VARs and DCC-type models (Diebold & Yilmaz, 2012; Engle, 2002). Volatility studies detect clustering and asymmetric responses to shocks using EGARCH across Australian cities, with determinants differing by location (Lee, 2009). Wavelet methods provide time–frequency decompositions to study co-movements and lead–lag relations in multiple scales (Torrence & Compo, 1998). Recent applications to housing markets and uncertainty indicators use wavelets and connectedness to capture multi-scale interactions; similar designs inform studies on Germany and Asian markets with policy uncertainty and financial stress measures (Kirikkaleli et al., 2021; Paul et al., 2024).

Within-country heterogeneity is addressed through city-tier or spatial models. A VAR study of China's first-, second-, and third-tier cities finds a negative interest-rate impact that diminishes by tier, mixed inflation effects over horizons, and positive growth effects, with bidirectional linkages between prices and inflation (Zhang, Li, Hui, & Li, 2016). Spatial hedonic analysis for Beijing shows that structural attributes and access to amenities vary in effect across space, complementing macro channels identified in the VAR (Duan et al., 2021). Cross-sectional evidence for Baku identifies location, size, repair level, and legal status as major price determinants for flats, with

room count relevant for houses and spatial gradients in land intensity (Aliyev, Amiraslanova, Bakirova, & Eynizada, 2019).

Evidence from emerging and small open economies highlights differences in transmission. For Turkey, monetary aggregates play a larger role in housing investment than employment, and shocks to interest rates, output, and prices affect housing activity (Sari et al., 2014). For Lithuania, a broad screen of 137 external factors identifies GDP growth, consumer spending, and household cash and deposits as key indicators, with effects varying by cycle stage (Stundzienė, Pilinkienė, & Grybauskas, 2022). For Kenya, ARDL estimates show that income, GDP, inflation, and exchange rates affect prices in both the short and long run; sales respond to income, rates, capital inflows, and exchange rates; rents respond to income, GDP, rates, and exchange rates (Okuta, Kivaa, Kieti, & Okaka, 2024).

The literature establishes: (i) long-run relations between housing prices and macro fundamentals; (ii) central roles for policy rates, credit, money, and exchange rates; (iii) dynamic, regime-dependent, and time-varying dependence; (iv) volatility clustering and asymmetric responses; and (v) spatial heterogeneity across city tiers and regions. Methods span cointegration/VECM, VAR and variance decompositions, Markov-switching models, EGARCH, wavelet coherence, and time-varying connectedness. These results motivate a combined approach that measures frequency-specific co-movements, evolving spillovers, conditional correlations, and asymmetric long-run effects. Applying this integrated framework to India can map linkages across horizons, evaluate the role of economic policy uncertainty, and relate market-based daily signals to quarterly macro adjustments.

3. Methodology

This study combines time–frequency and time-varying approaches on two datasets. Daily series are used to analyse co-movements, spillovers, and conditional correlations through wavelet coherence, a time-varying parameter VAR (TVP-VAR) with generalized forecast-error variance decompositions, and a DCC-GARCH specification. Quarterly series are used to estimate short-run and long-run asymmetric effects with a nonlinear ARDL (NARDL) model based on partial-sum decompositions. For wavelet coherence, the complex Morlet wavelet is used; significance is assessed against an AR(1) red-noise null with Monte Carlo methods, and the cone of influence is reported. The TVP-VAR is estimated via Kalman filtering with drifting coefficients and stochastic volatilities; connectedness is summarized by the total spillover index, directional "to/from," and net measures derived from generalized decompositions. The DCC-GARCH procedure estimates univariate GARCH(1,1) models for each series, standardizes residuals, and updates the dynamic correlation matrix with DCC(1,1); quasi-maximum likelihood is used for consistency under non-normality. The quarterly NARDL follows the bounds-testing approach to cointegration; lag orders are selected by AIC with small-sample correction, and Wald tests evaluate long-run and short-run asymmetry. All models include deterministic components as indicated by information criteria and undergo standard post-estimation diagnostics for residual autocorrelation, conditional heteroskedasticity, and parameter stability.

3.1. Data and sample

The sample spans January 2012 to March 2025. The effective sample for each model equals the intersection of available observations after alignment and transformations. Two frequency blocks are constructed and analysed separately. The daily block uses a real estate sector equity index

(RESI) as a market-based proxy for housing-sector valuations, together with the NIFTY50 index, the USD/INR spot rate, the 91-day Treasury bill yield, and an inflation proxy obtained by linearly interpolating the all-groups CPI from monthly to daily calendar dates and then merging to trading days. After merging by date, observations with missing values are removed listwise. Log levels are used for wavelet coherence; log returns of RESI, NIFTY50, and USD/INR, the first difference of the daily-interpolated log CPI, and the first difference of the Treasury bill yield (percentage points) are used where stationarity is required for TVP-VAR and DCC-GARCH. The quarterly block comprises the all-India Housing Price Index (HPI), real GDP, CPI, the 91-day Treasury bill rate averaged by quarter, and the India Economic Policy Uncertainty (EPU) index averaged by quarter when higher-frequency values exist. HPI, GDP, and CPI enter in natural logarithms, with differences used as indicated by unit-root tests; the Treasury bill rate enters in percentage points; EPU enters in levels or logarithms depending on stationarity diagnostics. All series are sourced from the National Stock Exchange of India (equity indices), the Reserve Bank of India (CPI, Treasury bill rate, USD/INR, HPI, GDP), and the policy uncertainty database for EPU. Table 1 lists variables, proxies, frequency, and sources.

Table 1. Variables, proxies, frequency, and sources

Frequency	Variable		Proxy / Definition	Source
Daily	Real estate sector index return	*RESI*	Real Estate Sector Index	NSE
Daily	Broad equity market (Index return)	*NIFTY50*	NIFTY50 daily closing value	NSE
Daily	Exchange rate (return)	*USDINR*	USD/INR daily spot rate	RBI
Daily	Interest rate	*TBILL*	91-day Treasury bill yield (daily observation)	RBI
Daily	Inflation	*Inflation*	CPI (All-Groups, India) linearly interpolated to daily calendar dates, merged to trading days	RBI
Quarterly	Housing prices	*HPI*	Housing Price Index (All-India)	RBI
Quarterly	Output	*lnGDP*	Real Gross Domestic Product (natural logarithm)	RBI
Quarterly	Interest rate	*Tbill*	91-day Treasury bill rate (quarterly average)	RBI
Quarterly	Price level	*CPI*	CPI (All-Groups, India)	RBI
Quarterly	Policy uncertainty	*EPU*	Economic Policy Uncertainty index (quarterly mean)	policyuncertainty.com

In both blocks, the calendar alignment is explicit. For daily models, CPI interpolation uses end-of-month anchors; interest rates and exchange rates follow their recorded dates and are not forward-

filled over non-trading days. For quarterly models, all series are aligned to standard calendar quarters; when a component is observed at higher frequency, it is aggregated by arithmetic averaging within the quarter. Prior to estimation, each series is screened for structural breaks and definitional changes documented by the source institutions; unit-root tests appropriate to the frequency and transformation determine the inclusion of differences and deterministic terms. These procedures ensure that the daily block can identify high-frequency co-movements and spillovers, while the quarterly block can identify long-run relations and asymmetric adjustments.

3.2. TVP-VAR connectedness for return spillovers

We estimate time-varying return spillovers using the TVP-VAR connectedness framework, which extends the VAR-based measures of Diebold and Yılmaz (2009, 2012, 2014). The dynamic specification follows Antonakakis et al. (2020), estimated via the Kalman filter to avoid arbitrary window selection and loss of initial observations. In line with Antonakakis et al. (2018), Gabauer and Gupta (2018), and Bouri et al. (2021), a TVP-VAR(1) chosen by BIC is specified as

$$Z_t = B_t Z_{t-1} + U_t \qquad U_t \sim N(0, S_t) \tag{1}$$

$$vec(B_t) = vec(B_{t-1}) + v_t \qquad v_t \sim N(0, R_t) \tag{2}$$

where Z_t and Z_{t-1} , are $k \times 1$ vectors of endogenous variables, B_t and S_t are $k \times k$ coefficient and covariance matrices, $vec(B_t)$ is a $k^2 \times 1$, and R_t is a $k^2 \times k^2$.

Generalised forecast error variance decompositions (GFEVDs) are computed following Koop et al. (1996) and Pesaran and Shin (1998). Unlike orthogonalised FEVDs, GFEVDs are invariant to ordering. The H-step-ahead GFEVD is

$$\phi_{ij,t}^{g}(H) = \frac{S_{ii}^{-1}\sum_{t=1}^{H-1}(e_i' A_t S_t e_j)^2}{\sum_{j=1}^{k}\sum_{t=1}^{H-1}(e_i' A_t S_t e_j)} \quad (3)$$

where e_i is a selection vector with unity in the i[th] position and zeros elsewhere. The GFEVD is normalised so that each row sums to unity:

$$\tilde{\phi}_{ij,t}^{g}(H) = \frac{\phi_{ij,t}^{g}(H)}{\sum_{j=1}^{k}\phi_{ij,t}^{g}(H)} \quad (4)$$

From the normalised GFEVD, the connectedness measures are:

$$TO_{jt} = \sum_{i=1,i\neq j}^{k}\tilde{\phi}_{ij,t}^{g}(H) \quad (5)$$

$$FROM_{jt} = \sum_{i=1,i\neq j}^{k}\tilde{\phi}_{ji,t}^{g}(H) \quad (6)$$

$$NET_{jt} = TO_{jt-}FROM_{jt} \quad (7)$$

$$TCI_t = \frac{1}{k}\sum_{j=1}^{k} TO_{jt} = \frac{1}{k}\sum_{j=1}^{k} FROM_{jt} \quad (8)$$

$$NPDC_{ij,t} = \tilde{\phi}_{ij,t}^{g}(H) - \tilde{\phi}_{ji,t}^{g}(H) \quad (9)$$

These statistics summarise magnitudes and directions of spillovers in the network.

3.3. DCC-GARCH connectedness for volatility spillovers

To model time-varying conditional volatilities and dynamic conditional correlations, we apply the Dynamic Conditional Correlation GARCH model of Engle (2002) and Engle and Sheppard (2001). The DCC-GARCH(1,1) is specified as

$$y_t = \mu_t + \epsilon_t, \qquad \epsilon_t \mid F_{t-1} \sim N(0, H_t) \quad (10)$$

$$\epsilon_t = H_t^{\frac{1}{2}} u_t, \qquad u_t \sim N(0, I) \tag{11}$$

$$H_t = D_t R_t D_t \tag{12}$$

where F_{t-1} denotes the information set available at $t-1$. Here, y_t, μ_t, ϵ_t and u_t are $N \times 1$; H_t is the $N \times N$ conditional variance–covariance matrix, R_t is the dynamic conditional correlation matrix, and $D_t = diag\left(h_{11t}^{\frac{1}{2}}, \dots, h_{NN}^{\frac{1}{2}}\right)$ is the diagonal matrix of conditional standard deviations.

Stage one estimates D_t via univariate GARCH(1,1) for each series (Bollerslev, 1986):

$$h_{ii,t} = \omega + \alpha \epsilon_{i,t-1}^2 + \beta h_{ii,t-1}; \qquad \omega > 0, \alpha \geq 0 \text{ and } \beta \geq 0. \tag{13}$$

In the second step, dynamic correlations follow:

$$R_t = diag\left(q_{ii,t}^{-\frac{1}{2}}, \dots, q_{NN,t}^{-\frac{1}{2}}\right) Q_t diag\left(q_{ii,t}^{-\frac{1}{2}}, \dots, q_{NN,t}^{-\frac{1}{2}}\right) \tag{14}$$

$$Q_t = (1 - a - b)\bar{Q} + a u_{t-1} u_{t-1}' + b Q_{t-1} \tag{15}$$

where $\bar{Q}$ is the unconditional covariance of the standardized residuals u_t. Multi-step forecasts under DCC are (Gabauer, 2020)

$$E\left(h_{ii,t+h} \mid F_t\right) = \sum_{i=0}^{h-1} \omega(\alpha + \beta)^i + (\alpha + \beta)^{h-1} E\left(h_{ii,t+h-1} \mid F_t\right), h > 1 \tag{16}$$

$$E(Q_{t+h} \mid Ft) = (1 - a - b)\bar{Q} + aE(u_{t+h-1} u_{t+h-1}' \mid F_t) + bE(Q_{t+h-1} \mid F_t), h > 1 \tag{17}$$

$$E(H_{t+h} \mid F_t) \approx E(D_{t+h} \mid F_t) E(R_{t+h} \mid F_t) E(D_{t+h} \mid F_t) \tag{18}$$

Volatility spillovers are evaluated via the generalized forecast-error variance decomposition (GFEVD) based on generalized impulse responses $\tilde{\phi}_{ij,t}^{g}(J)$ (Gabauer, 2020). The J-step normalized GFEVD entry is

$$\tilde{\phi}_{ij,t}^{g}(J) = \frac{\sum_{h=1}^{j=1}\left(\Psi_{ij,t}^{g}(h)\right)^{2}}{\sum_{J=1}^{N}\sum_{h=1}^{j=1}\left(\Psi_{ij,t}^{g}(h)\right)^{2}} \tag{19}$$

so that $\sum_{J=1}^{N}\tilde{\phi}_{ij,t}^{g}(J) = 1$ for each i The Total Connectedness Index is

$$C_{t}^{g}(J) = \frac{1}{N}\sum_{i,j=1,i\neq j}^{N}\tilde{\phi}_{ij,t}^{g}(J) \tag{20}$$

Directional measures are defined as the shares to and from others:;

$$C_{i\rightarrow j,t}^{g}(J) = \frac{\sum_{j=1,i\neq j}^{N}\tilde{\phi}_{ji,t}^{g}(J)}{\sum_{j=1}^{N}\tilde{\phi}_{ji,t}^{g}(J)} \tag{21}$$

$$C_{i\leftarrow j,t}^{g}(J) = \frac{\sum_{j=1,i\neq j}^{N}\tilde{\phi}_{ij,t}^{g}(J)}{\sum_{i=1}^{N}\tilde{\phi}_{ij,t}^{g}(J)} \tag{22}$$

with net connectedness:

$$C_{i,t}^{g} = C_{i\rightarrow j,t}^{g}(J) - C_{i\leftarrow j,t}^{g}(J) \tag{23}$$

and the net pairwise directional connectedness:

$$NPDC_{i,j}(J) = \tilde{\phi}_{ji,t}^{g}(J) - \tilde{\phi}_{ij,t}^{g}(J) \tag{24}$$

A positive $NPDC_{i,j}(J)$ indicates that i transmits more volatility to j than it receives from j (Gabauer, 2020).

3.4. Wavelet coherence for time–frequency spillovers

Wavelet coherence is used to measure local correlation in the joint time–frequency domain and is suitable for non-stationary economic series (Gençay et al., 2001; Percival & Walden, 2000; Torrence & Compo, 1998). In this study, coherence is computed only for pairs identified as most relevant by the TVP-VAR connectedness analysis. The mother wavelet $\psi(t)$ generates the location–scale family

$$\psi_{u,s}(t) = \frac{1}{\sqrt{s}}\psi\left(\frac{t-u}{s}\right) \tag{25}$$

with location u and scale $s > 0$.The admissibility condition,

$$C_\psi = \int_0^\infty \frac{|\Psi(f)|^2}{f} df < \infty \tag{26}$$

where $\Psi(f)$ is the Fourier transform of $\psi(t)$, ensures reconstruction. The Morlet wavelet is adopted,

$$\psi^M(t) = \frac{1}{\pi^{1/4}} e^{i\omega_0 t} e^{-t^2/2} \quad , \quad \omega_0 = 6 \tag{27}$$

as commonly used in economic applications (Aguiar-Conraria et al., 2008; Rua & Nunes, 2009). The continuous wavelet transforms (CWT) of $x(t)$ is

$$W_x(u,s) = \int_{-\infty}^{\infty} x(t) \frac{1}{\sqrt{s}} \psi\left(\frac{t-u}{s}\right) dt \tag{28}$$

with inverse

$$x(t) = \frac{1}{C_\psi}\int_0^\infty \left[\int_{-\infty}^{\infty} W_x(u,s)\psi_{u,s}(t)\,du\right]\frac{ds}{s^2}\,, s > 0 \tag{29}$$

and energy preservation

$$\|x\|^2 = \frac{1}{C_\psi}\int_0^\infty \left[\int_{-\infty}^{\infty} |W_x(u,s)|^2\,du\right]\frac{ds}{s^2} \tag{30}$$

For two series $x(t)$ and $y(t)$ is the cross-wavelet transform is

$$W_x(u,s) = W_x(u,s)W_y^*(u,s) \tag{31}$$

and the squared wavelet coherence is

$$R^2(u,s) = \frac{\left|S\left(s^{-1}W_{xy}(u,s)\right)\right|^2}{S(s^{-1}|W_x(u,s)|^2)S\left(s^{-1}|W_y(u,s)|^2\right)} \tag{32}$$

where $S(\cdot)$ denotes a smoothing in time and scale, and $R^2(u,s) \in [0,1]$. Phase differences are.

$$\varphi_{xy}(u,s) = tan^{-1}\left(\frac{Im\left[S\left(s^{-1}W_{xy}(u,s)\right)\right]}{Re\left[S\left(s^{-1}W_{xy}(u,s)\right)\right]}\right) \tag{33}$$

which indicate lead–lag relations: rightward arrows denote in-phase comovement, leftward anti-phase; upward (downward) arrows indicate $x(t)$ leading $y(t)$, ($y(t)$ *leading* $x(t)$) by 90°. Statistical significance is assessed by Monte Carlo procedures (Grinsted et al., 2004; Torrence & Webster,

1999), and the cone of influence is used to delimit regions affected by edge effects (Torrence & Compo, 1998).

3.5. NARDL for long-run and asymmetric relations

Quarterly data are used to estimate a nonlinear autoregressive distributed-lag model that allows for long-run cointegration and short-run asymmetry (Pesaran, Shin, & Smith, 2001; Shin, Yu, & Greenwood-Nimmo, 2014). Let $y_t = (HPI_t)$ and $x_{1,t} = \ln(GDP_t),\ and\ x_{2,t} = (Tbill_t)$ (percent), $x_{4,t} = EPU_t$. For each regressor $x_{j,t}$ we construct partial-sum processes

$x_{j,t}^{+} = \sum_{s=1}^{t} \Delta x_{j,s}^{+}$, $x_{j,t}^{-} = \sum_{s=1}^{t} \Delta x_{j,s}^{-}$, $\Delta x_{j,s}^{+} = \max(\Delta x_{j,s}, 0)$, $\Delta x_{j,s}^{-} = \min(\Delta x_{j,s}, 0)$, so that $x_{j,t} = x_{j,0} + x_{j,0}^{+} + x_{j,0}^{-}$ (Shin et al., 2014). The NARDL $(p, q_1, \dots, q_4)$ in conditional error-correction form is

$$\Delta y_t = \varphi \left[y_{t-1} - \sum_{j=1}^{4} \beta_j^{+} x_{j,t-1}^{+} - \sum_{j=1}^{4} \beta_j^{-} x_{j,t-1}^{-} \right] + \sum_{i=1}^{p-1} \rho_i \Delta y_{t-i} + \sum_{j=1}^{4} \left(\sum_{i=0}^{q_j - 1} \pi_{j,i}^{+} \Delta x_{j,t-i}^{+} + \sum_{i=0}^{q_j - 1} \pi_{j,i}^{-} \Delta x_{j,t-i}^{-} \right) + \varepsilon_i \quad (34)$$

with $\varphi < 0$ for stability. The long-run asymmetric coefficients are obtained from the levels parameters as $\beta_j^{+} = -\frac{\theta_j^{+}}{\varphi}$, $\beta_j^{-} = -\frac{\theta_j^{-}}{\varphi}$, when θ_j^{+} and θ_j^{-} are the coefficients on $x_{j,t-i}^{+}$ and $x_{j,t-i}^{-}$ in the levels part of the model (Shin et al., 2014). Lag orders (p, q_j) are selected by information criteria within a quarterly-appropriate upper bound (e.g., four lags).

Cointegration is assessed by the bounds test of Pesaran et al. (2001) using the joint null of no long-run relationship, $H_0: \theta_y = \theta_1^+ = \theta_1^- = \cdots = \theta_4^+ = \theta_4^- = 0$, against the alternative that at least one level coefficient is non-zero. Critical values are drawn from the $I(0) - I(1)$ bounds; the procedure requires that no variable is I(2). Long-run asymmetry is tested by Wald tests of $H_0: \beta_j^+ = \beta_j^-$ for each j; short-run asymmetry is tested by $H_0: \sum_{i=0}^{q_j-1} \pi_{j,i}^+ = \sum_{i=0}^{q_j-1} \pi_{j,i}^-$ (Shin et al., 2014).

Dynamic multipliers trace the adjustment of y_t to partial-sum shocks in $x_{j,t}$. For horizon $h = 0,1, \ldots,$

$m_{j,h}^+ = \sum_{s=0}^{h} \frac{\partial y_{t+s}}{\partial x_{j,t}^+}$, $m_{j,h}^- = \sum_{s=0}^{h} \frac{\partial y_{t+s}}{\partial x_{j,t}^-}$ with limits $m_{j,\infty}^+ = \beta_j^+$ and $m_{j,\infty}^- = \beta_j^-$ (Shin et al., 2014). Model adequacy is examined through serial-correlation and heteroskedasticity diagnostics and parameter-stability tests; inference is conducted under the standard assumptions for ARDL estimators (Pesaran et al., 2001).

4. Results

This section reports results from the two-stage design. The primary analysis uses daily series to summarize distributional properties, dependence, and connectedness. The secondary analysis uses quarterly series to estimate long-run and asymmetric responses. All variables and sources are defined in Table 1.

4.1. Primary analysis: daily data

4.1.1. Descriptive statistics

Table 2 shows distributional diagnostics and Kendall rank correlations for the daily series over January 2012–March 2025. Mean returns are close to zero; skewness and excess kurtosis indicate non-normality, and Jarque–Bera rejects normality for all series. The ERS tests support stationarity

of returns series of RESI, NIFTY50, and USDINR. Ljung–Box statistics for levels and squares indicate serial correlation and conditional heteroskedasticity. Kendall correlations show a positive association between RESI and NIFTY50 (0.456) and negative associations between equity returns and USDINR (−0.156 and −0.200), while links with Inflation and TBill are weak.

Table 2. Descriptive statistics, diagnostics, and Kendall correlations (daily data, 2012–2025)

	RESI	Inflation	TBILL	NIFTY50	USDINR
Mean	0.000	0.005***	0.063***	0.000**	0.000**
	(0.384)	(0.000)	(0.000)	(0.028)	(0.012)
Variance	0.000	0.000	0.000	0.000	0.000
Skewness	-0.521***	1.081***	-0.203***	-1.351***	0.538***
	(0.000)	(0.000)	(0.000)	(0.000)	(0.000)
Ex.Kurtosis	3.282***	4.869***	0.141	23.127***	10.810***
	(0.000)	(0.000)	(0.125)	(0.000)	(0.000)
JB	1459.546***	3492.512***	22.743***	66706.554***	14520.030***
	(0.000)	(0.000)	(0.000)	(0.000)	(0.000)
ERS	-22.683	-1.045	-0.571	-12.336	-4.145
	(0.000)	(0.096)	(0.086)	(0.000)	(0.000)
Q(20)	28.272***	18725.480***	30402.191***	66.069***	34.108***
	(0.000)	(0.000)	(0.000)	(0.000)	(0.000)
Q^2(20)	211.562***	15055.326***	29867.245***	777.053***	1764.263***
	(0.000)	(0.000)	(0.000)	(0.000)	(0.000)
Kendall	RESI	Inflation	TBILL	NIFTY50	USDINR
RESI	1.000***	0.005	-0.022	0.456***	-0.156***
Inflation	0.005	1.000***	0.003	0.018	-0.002
TBILL	-0.022	0.003	1.000***	-0.020	0.008
NIFTY50	0.456***	0.018	-0.020	1.000***	-0.200***
USDINR	-0.156***	-0.002	0.008	-0.200***	1.000***

*p-values in parentheses. JB = Jarque–Bera; ERS = Elliott–Rothenberg–Stock DF-GLS; Q(20) = Ljung–Box for returns; Q^2(20) = Ljung–Box for squared returns. Significance: *** p<0.01, ** p<0.05.*

4.1.2. TVP VAR Connectedness approach results for return spillovers

Table 3 reports the average generalized forecast-error variance decomposition from the TVP-VAR. Rows show the shares of each variable's forecast-error variance from shocks in the column variables (row sums of off-diagonals = FROM). The last row aggregates each column's to-others contribution (TO). NET is TO − FROM. The total connectedness index (TCI) equals the grand sum of off-diagonals divided by the number of variables; the table reports the current value and the sample average.

Equity market shocks transmit the largest share to others (TO for NIFTY50 = 41.70%), followed by RESI (37.09%) and USDINR (16.58%). Monetary variables transmit less (Inflation 6.21%, TBILL 4.81%). RESI and NIFTY50 display strong bilateral links (NIFTY50→RESI = 26.61; RESI→NIFTY50 = 27.76). USDINR receives net spillovers (NET = −4.19) and TBILL and Inflation are also net receivers. The system-wide connectedness is moderate (current TCI = 26.60%; average TCI = 21.28%).

Table 3. TVP-VAR connectedness matrix

	RESI	Inflation	TBILL	NIFTY50	USDINR	FROM
RESI	64.51	1.49	0.93	27.76	5.30	35.49
Inflation	2.25	93.10	1.08	2.11	1.46	6.90
TBILL	1.38	2.12	93.22	1.21	2.07	6.78
NIFTY50	26.61	1.30	0.82	63.53	7.74	36.47
USDINR	6.85	1.30	1.98	10.63	79.23	20.77
TO	37.09	6.21	4.81	41.70	16.58	106.40
Inc.Own	101.61	99.31	98.03	105.24	95.81	cTCI/TCI
NET	1.61	−0.69	−1.97	5.24	−4.19	26.60 / 21.28
NPT	3.00	1.00	0.00	4.00	2.00	

Notes: The Total Connectedness Index (TCI) is estimated using a TVP-VAR framework with a lag order of one, selected according to the Bayesian Information Criterion (BIC). The connectedness measures are obtained from the 20-step-ahead generalized forecast error variance decomposition.

Figures 1–5 summarize the time-varying connectedness. The Total Connectedness Index (Figure 1) varies over the sample with recurrent bursts, indicating shifts in aggregate spillovers. “FROM” measures (Figure 2) show that RESI and NIFTY50 receive larger shares than the macro series, with USDINR in an intermediate position and Inflation and TBILL comparatively small. “TO” measures (Figure 3) indicate that NIFTY50 and RESI are the main transmitters, while USDINR, Inflation, and TBILL contribute less and mostly in short episodes. The net measure (Figure 4) is positive for NIFTY50 and RESI for extended periods and negative for USDINR, with Inflation and TBILL generally net receivers; temporary sign reversals coincide with high TCI episodes. The network graph (Figure 5) is consistent with Table 3: the strongest edges run from NIFTY50 to RESI and to USDINR, with additional transmission from RESI to USDINR and to Inflation, and a weaker link toward TBILL.

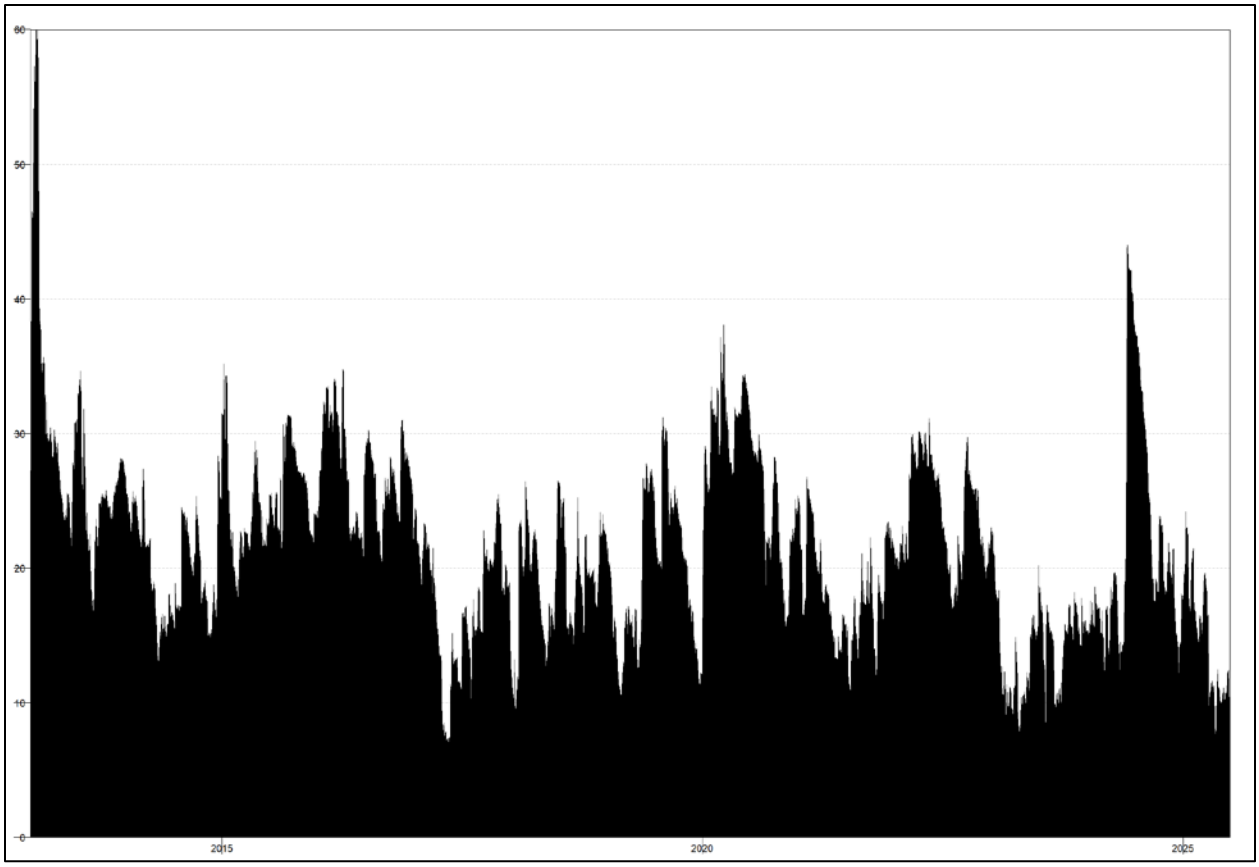

Figure 1. Total Connectedness Index (TCI), TVP-VAR (daily data: RESI, NIFTY50, USDINR, TBILL, Inflation; Jan 2012–Mar 2025).

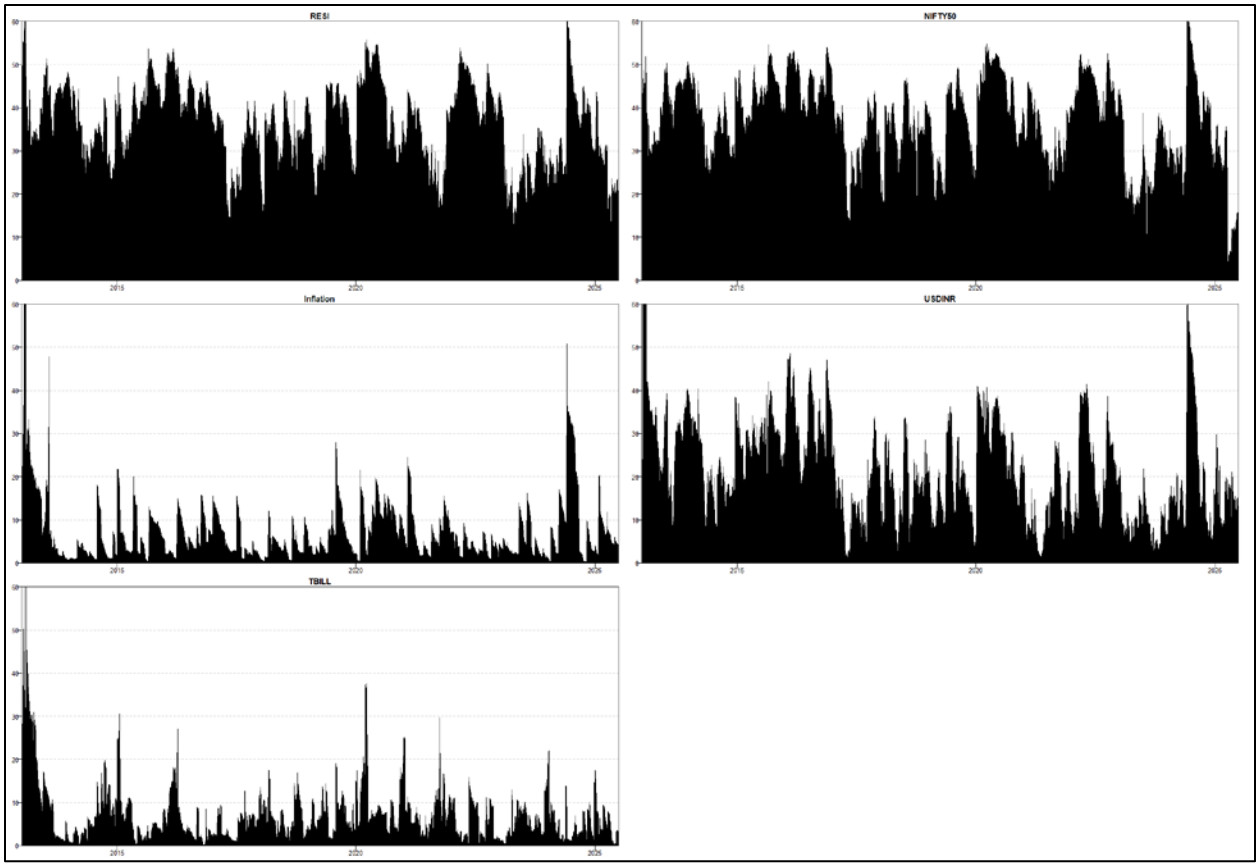

Figure 2. Directional Connectedness FROM Others by Variable, TVP-VAR (daily data, 2012–2025).

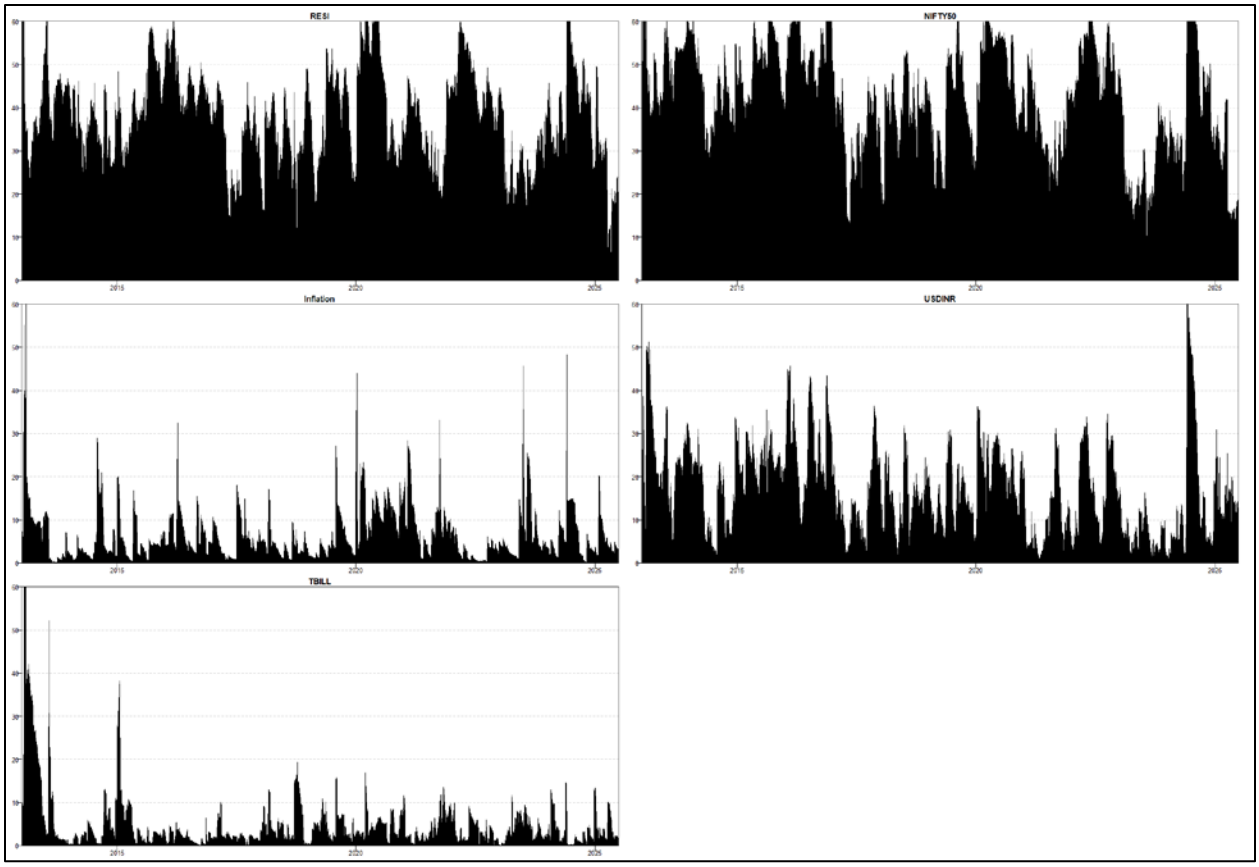

Figure 3. Directional Connectedness TO Others by Variable, TVP-VAR (daily data, 2012–2025).

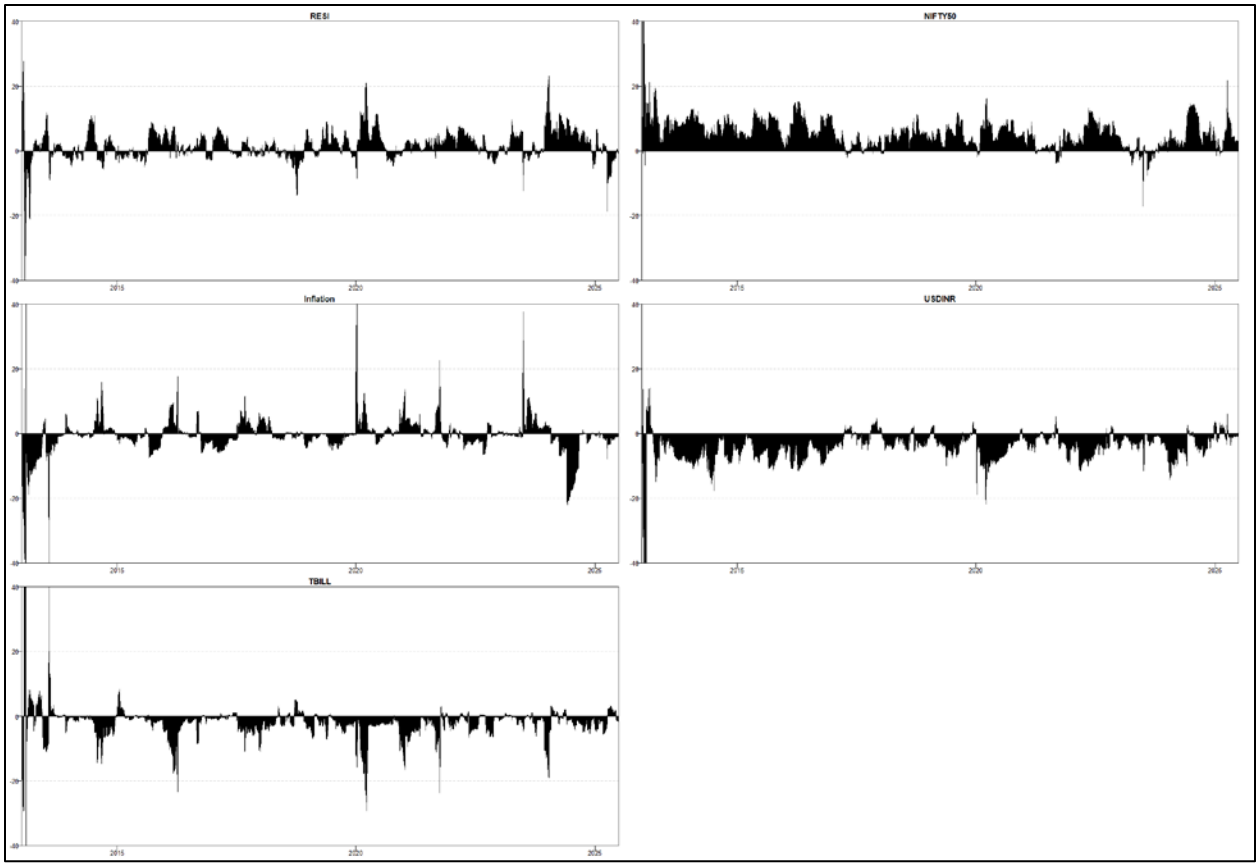

Figure 4. Net Total Directional Connectedness (TO − FROM) by Variable, TVP-VAR (daily data, 2012–2025).

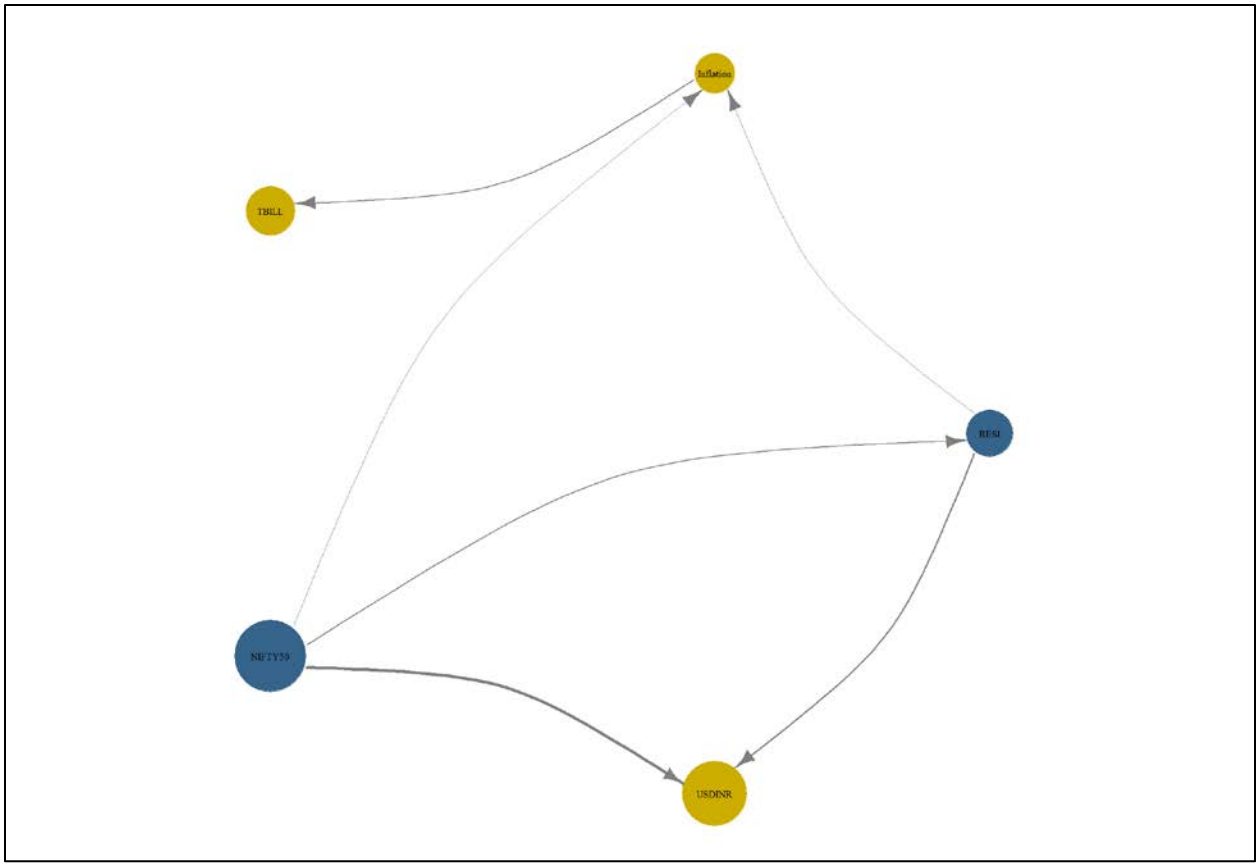

Figure 5. Connectedness Network Graph (average GFEVD; arrows indicate direction of net transmission), TVP-VAR (daily data, 2012–2025).

Note for figure 1-5: Estimates are obtained from a TVP-VAR(1) selected by BIC with a 20-step-ahead generalized forecast-error variance decomposition. The red series depicts the Diebold–Yılmaz (2012) benchmark based on a 200-day rolling-window VAR(1) (BIC) using the same 20-step-ahead generalized decomposition.

4.1.3. DCC GARCH connectedness results for volatility spillovers

Table 4 summarizes volatility spillovers from the DCC-GARCH–based GFEVD. The largest transmission "to others" arises from NIFTY50 (TO = 30.76%), followed by RESI (19.53%); USDINR transmits 7.63%, while Inflation and TBILL contribute negligibly. RESI receives more volatility than it transmits (FROM = 26.65%; NET = −7.12%), whereas NIFTY50 is a net transmitter (NET = 9.87%). USDINR is a net receiver (NET = −2.83%). The own shares on the diagonal indicate that Inflation and TBILL variances are almost entirely idiosyncratic (≈100%), and USDINR retains a high own component (89.54%). The system-wide connectedness is modest

relative to return spillovers, with the current TCI of 14.50% and a sample-average TCI of 11.60%. Figure 6 plots the time path of the TCI, and Figure 7 presents the corresponding network, which highlights dominant edges from NIFTY50 toward RESI and USDINR and weak links for Inflation and TBILL.

Table 4. DCC-GARCH connectedness matrix

	RESI	Inflation	TBILL	NIFTY50	USDINR	FROM
RESI	73.35	0.01	0.03	23.58	3.04	26.65
Inflation	0.00	99.99	0.01	0.00	0.00	0.01
TBILL	0.00	0.01	99.99	0.00	0.00	0.01
NIFTY50	16.26	0.03	0.00	79.12	4.59	20.88
USDINR	3.27	0.00	0.01	7.18	89.54	10.46
TO	19.53	0.05	0.05	30.76	7.63	58.02
Inc.Own	92.88	100.03	100.04	109.87	97.17	cTCI/TCI
NET	−7.12	0.03	0.04	9.87	−2.83	14.50 / 11.60
NPT	1.00	4.00	3.00	2.00	0.00	

Notes: Values reported are generalized forecast-error variance decompositions from 100-step-ahead forecasts of a DCC-GARCH model with a lag length of order 1, as determined by the Bayesian Information Criterion (BIC).

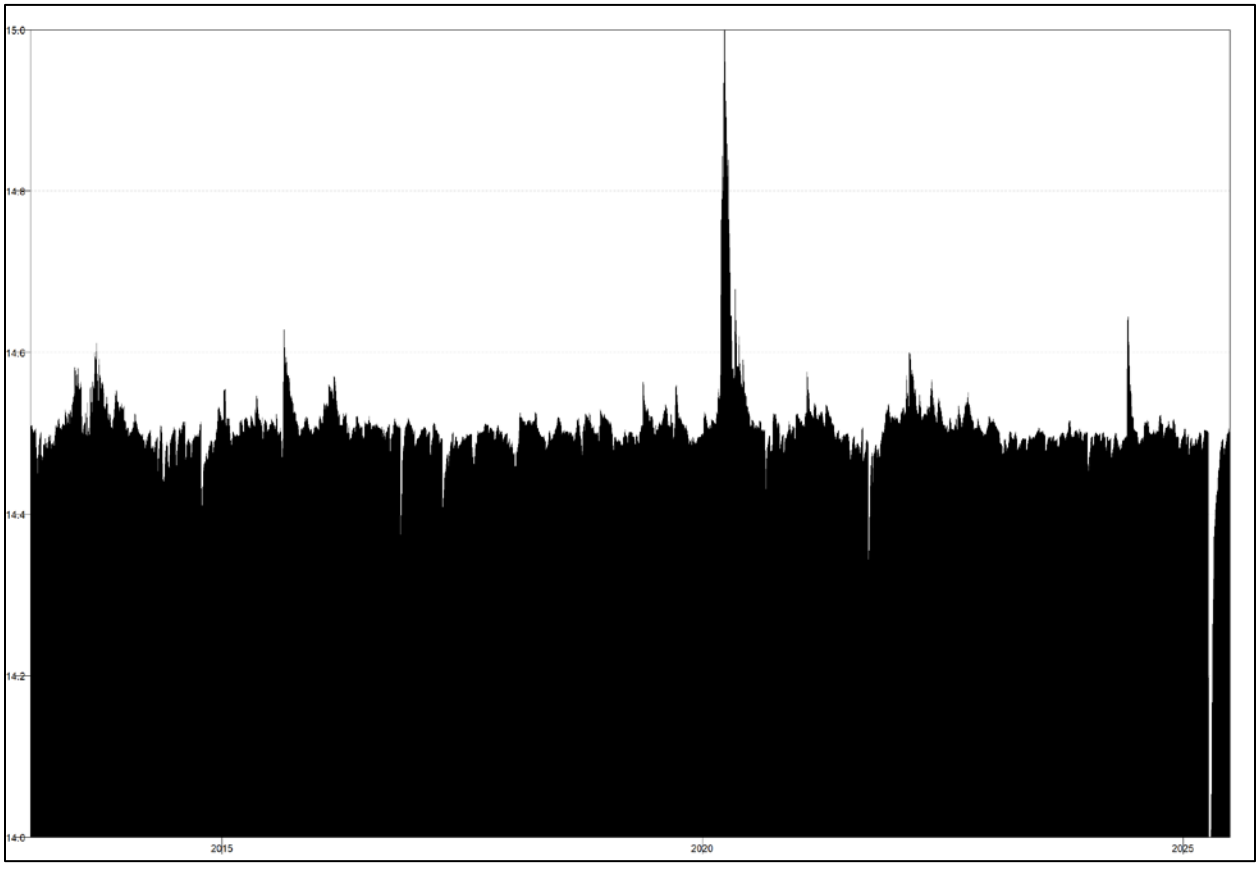

Figure 6. Total Connectedness Index (volatility), DCC-GARCH (daily data: RESI, NIFTY50, USDINR, TBILL, Inflation; Jan 2012–Mar 2025).

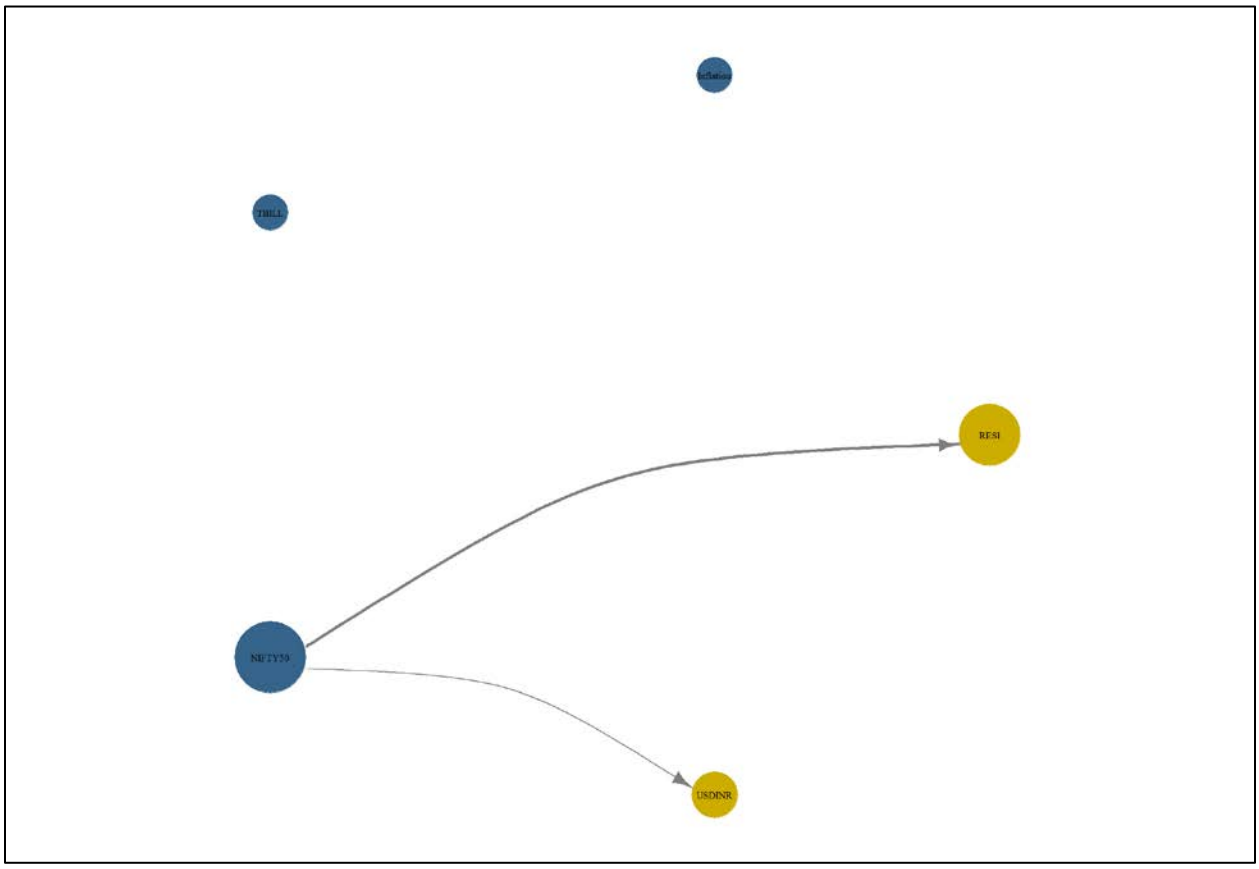

Figure 7. Volatility Connectedness Network (average GFEVD; arrows indicate direction of net transmission), DCC-GARCH (daily data, 2012–2025).

Notes for figure 6 and 7: Values reported are variance decompositions based on 100-day-ahead forecasts using DCC GARCH model with a lag length of order 1, as determined by the Bayesian Information Criterion (BIC).

4.1.4. Wavelet Coherence results

Wavelet coherence is computed for the daily pairs identified in the primary analysis. Coherence clusters are interpreted within the cone of influence and at scales that map to medium (≈16–128 trading days) and low frequencies (≥128 trading days). Figures 8–17 display the squared coherence surfaces and phase arrows.

For pairs with RESI, the coherence with NIFTY50 (Figure 10) is persistent at medium and low frequencies. Phase arrows are mostly rightward and, in several medium-frequency episodes, point upward, indicating in-phase comovement with NIFTY50 leading RESI in those intervals. RESI

and USDINR (Figure 11) exhibit coherent regions at medium and low frequencies with many leftward arrows, consistent with an anti-phase relationship; downward arrows in some segments indicate that USDINR leads RESI in those horizons. RESI and TBILL (Figure 9) show low-frequency coherence with many leftward arrows and upward directions from TBILL, indicating an anti-phase relation with TBILL leading at long cycles. RESI and Inflation (Figure 8) display intermittent coherence at medium to low frequencies with mixed phase directions, implying time-varying lead–lag patterns.

Among macro–financial pairs, Inflation–TBILL (Figure 12) displays low-frequency coherence with arrows largely rightward and, in places, upward from TBILL, indicating comovement with TBILL leading at long horizons. Inflation–NIFTY50 (Figure 13) shows episodic medium-frequency coherence with mixed phase directions. Inflation–USDINR (Figure 14) exhibits low-frequency coherence early and late in the sample, with downward arrows in several regions indicating USDINR leading Inflation. TBILL–NIFTY50 (Figure 15) has pronounced coherence at low frequencies with upward arrows from TBILL, indicating that TBILL leads NIFTY50 over long cycles. TBILL–USDINR (Figure 16) shows coherent regions at low frequencies with TBILL leading in several intervals. NIFTY50–USDINR (Figure 17) presents medium- and low-frequency coherence with many leftward arrows, consistent with an anti-phase relation; upward arrows from NIFTY50 in parts of the medium-frequency band indicate NIFTY50 leading USDINR during those episodes.

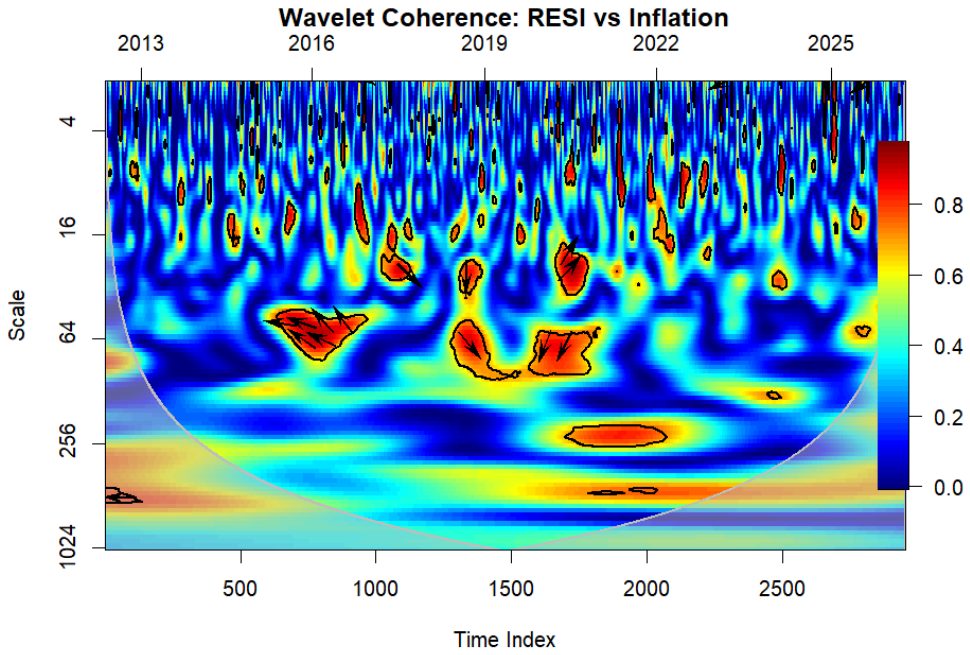

Figure 8. Wavelet Coherence: RESI vs Inflation.

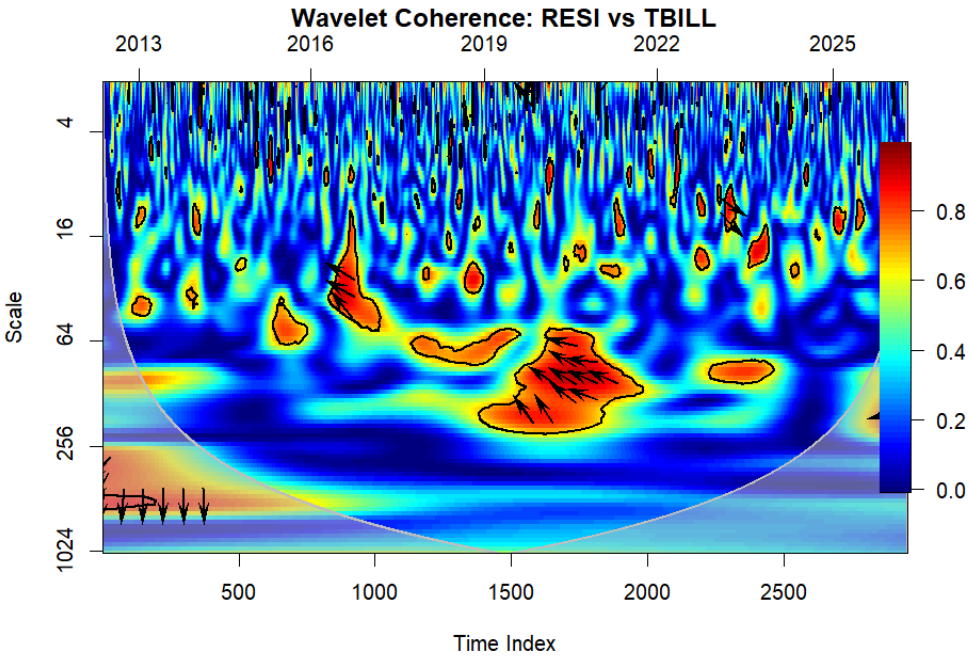

Figure 9. Wavelet Coherence: RESI vs TBILL.

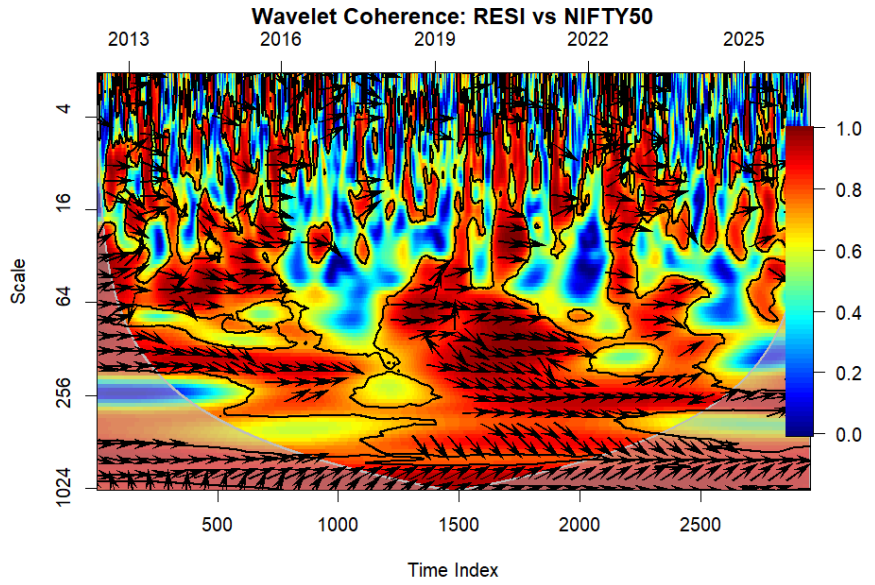

Figure 10. Wavelet Coherence: RESI vs NIFTY50.

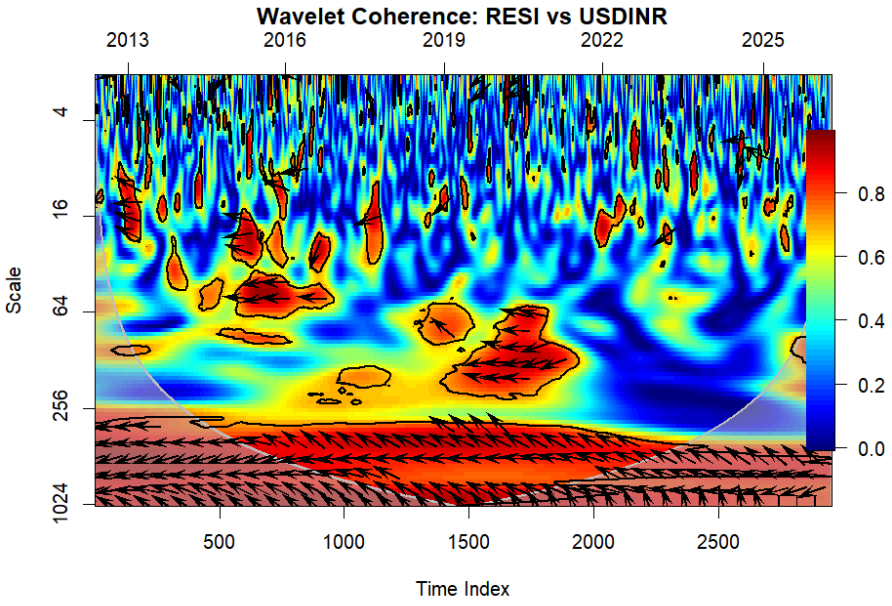

Figure 11. Wavelet Coherence: RESI vs USDINR.

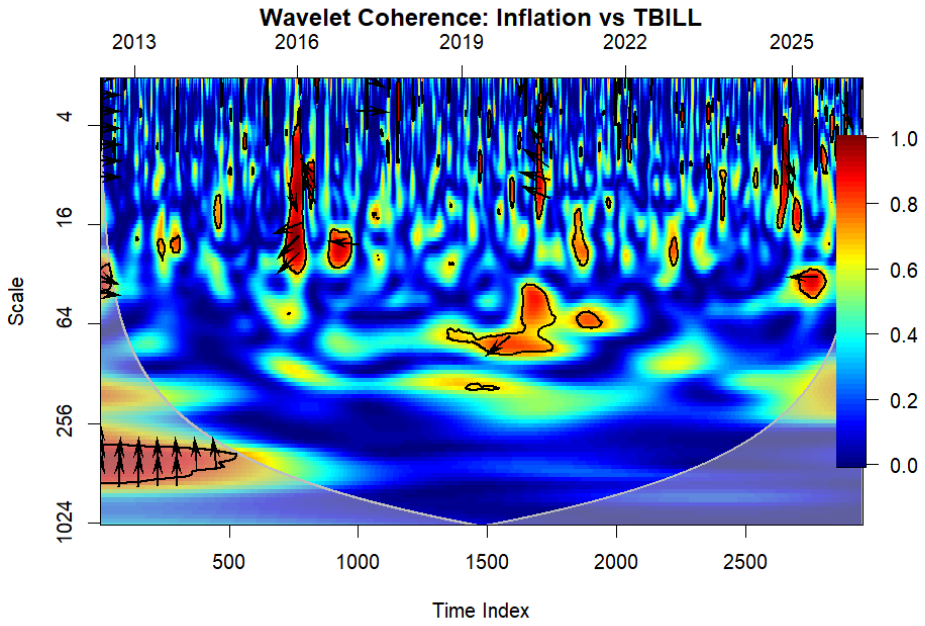

Figure 12. Wavelet Coherence: Inflation vs TBILL.

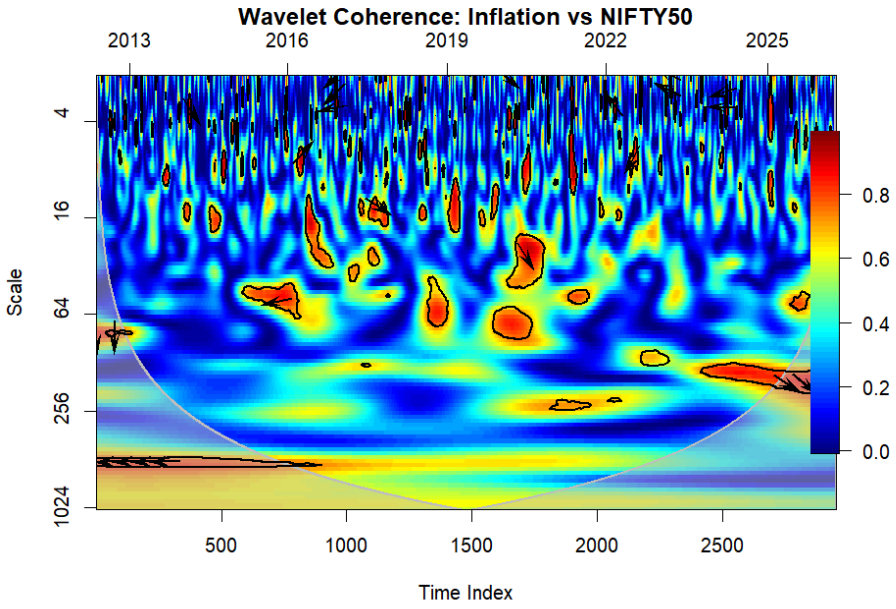

Figure 13. Wavelet Coherence: Inflation vs NIFTY50.

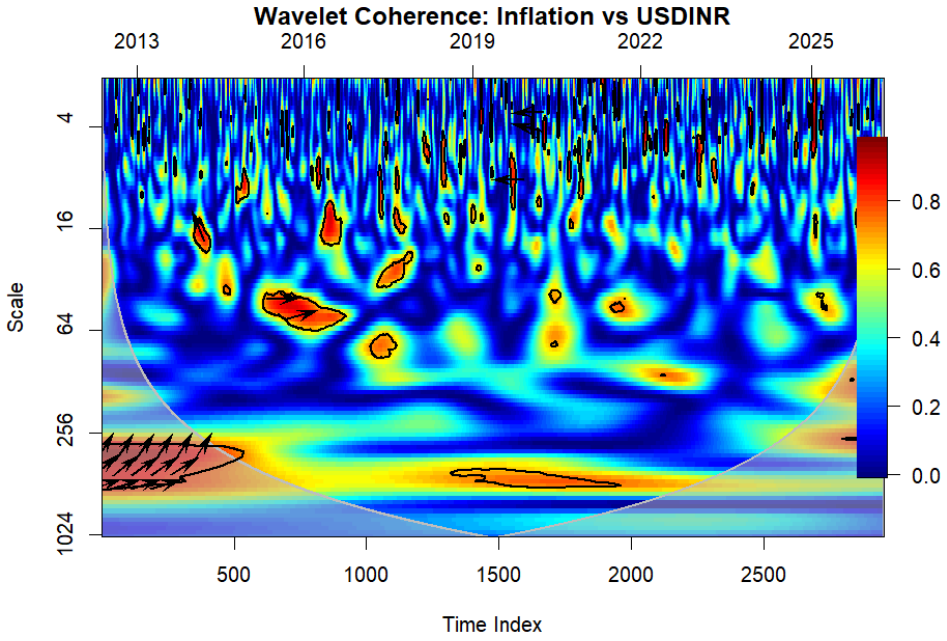

Figure 14. Wavelet Coherence: Inflation vs USDINR.

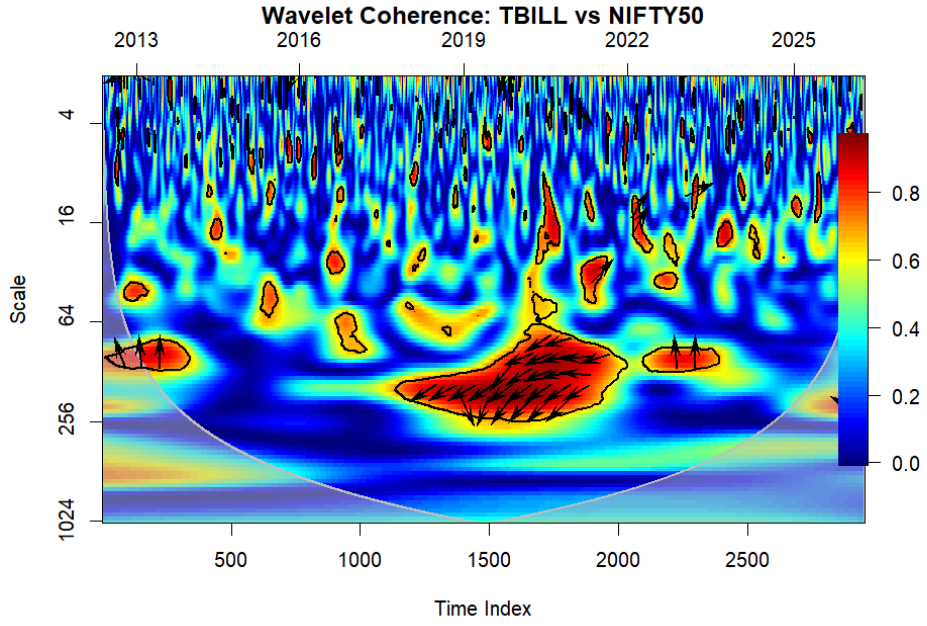

Figure 15. Wavelet Coherence: TBILL vs NIFTY50.

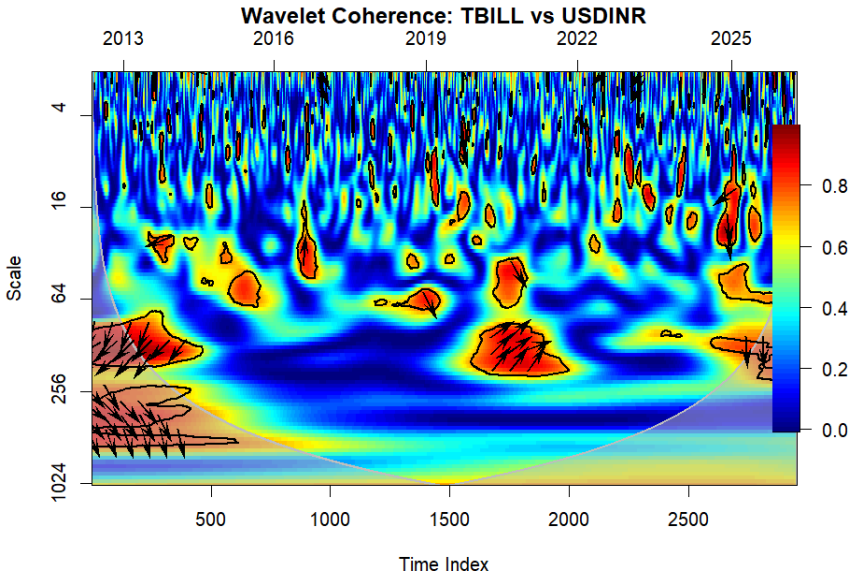

Figure 16. Wavelet Coherence: TBILL vs USDINR.

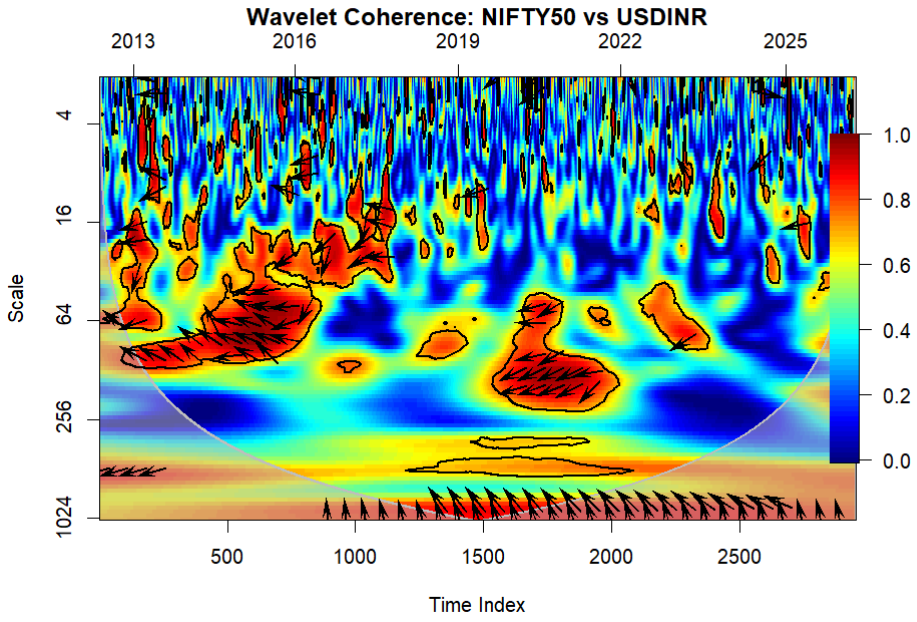

Figure 17. Wavelet Coherence: NIFTY50 vs USDINR.

4.2. Quarterly analysis: NARDL results

Figure 18 summarizes unconditional associations among the quarterly regressors. lnGDP and CPI are highly correlated (0.95), while Tbill is negatively correlated with both lnGDP (−0.53) and CPI (−0.54). EPU is moderately correlated with Tbill (0.41) and weakly related to lnGDP and CPI (−0.32 and −0.21). These patterns motivate an NARDL specification with partial-sum decompositions to allow asymmetric short-run effects and to separate level adjustment from contemporaneous movements.

Table 5 reports the NARDL estimates for ΔHPI with four autoregressive lags and contemporaneous positive/negative partial sums for lnGDP, Tbill, CPI and EPU. The lag structure on HPI is significant at the first two lags, indicating persistence in quarterly house price dynamics. Among the macroeconomic drivers, only increases in the short-term rate are significant: $Tbill_{pos,t}$ enters positively at the 5% level, while $Tbill_{neg,t}$ is not significant, implying short-run asymmetry for policy rate movements. Contemporaneous positive and negative components of lnGDP, CPI and EPU are not statistically different from zero at conventional levels. On balance, the quarterly results indicate inertia in HPI and asymmetric sensitivity to rate increases, with no detectable short-run effects from output, prices, or policy uncertainty in this specification.

Table 5. NARDL estimates for quarterly HPI (2012Q1–2025Q1)

Variable	Coefficient	Std. Error	z-Statistic	p-Value	Significance
const	27.8072	13.299	2.091	0.044	*
HPI.L1	0.3829	0.162	2.367	0.024	**
HPI.L2	0.4436	0.169	2.625	0.013	**
HPI.L3	−0.1456	0.169	−0.864	0.394	
HPI.L4	0.1455	0.167	0.871	0.390	
lnGDP_pos.L0	−11.9288	12.320	−0.968	0.340	
lnGDP_neg.L0	−0.7186	10.099	−0.071	0.944	
Tbill_pos.L0	205.2594	93.143	2.204	0.034	**
Tbill_neg.L0	9.3350	105.340	0.089	0.930	
CPI_pos.L0	−0.0729	0.255	−0.286	0.777	
CPI_neg.L0	−0.7942	0.839	−0.946	0.351	
EPU_pos.L0	0.0059	0.032	0.187	0.853	
EPU_neg.L0	−0.0640	0.047	−1.367	0.180	

*Notes: Significance codes: *** p<0.01, ** p<0.05, * p<0.10.*
"pos" and "neg" indicate the positive and negative partial-sum components of each regressor. "Lk" marks the k-th lag (for example, L1 is one quarter lag) and "L0" marks the contemporaneous effect; asterisks denote significance at the one, five, and ten percent levels.

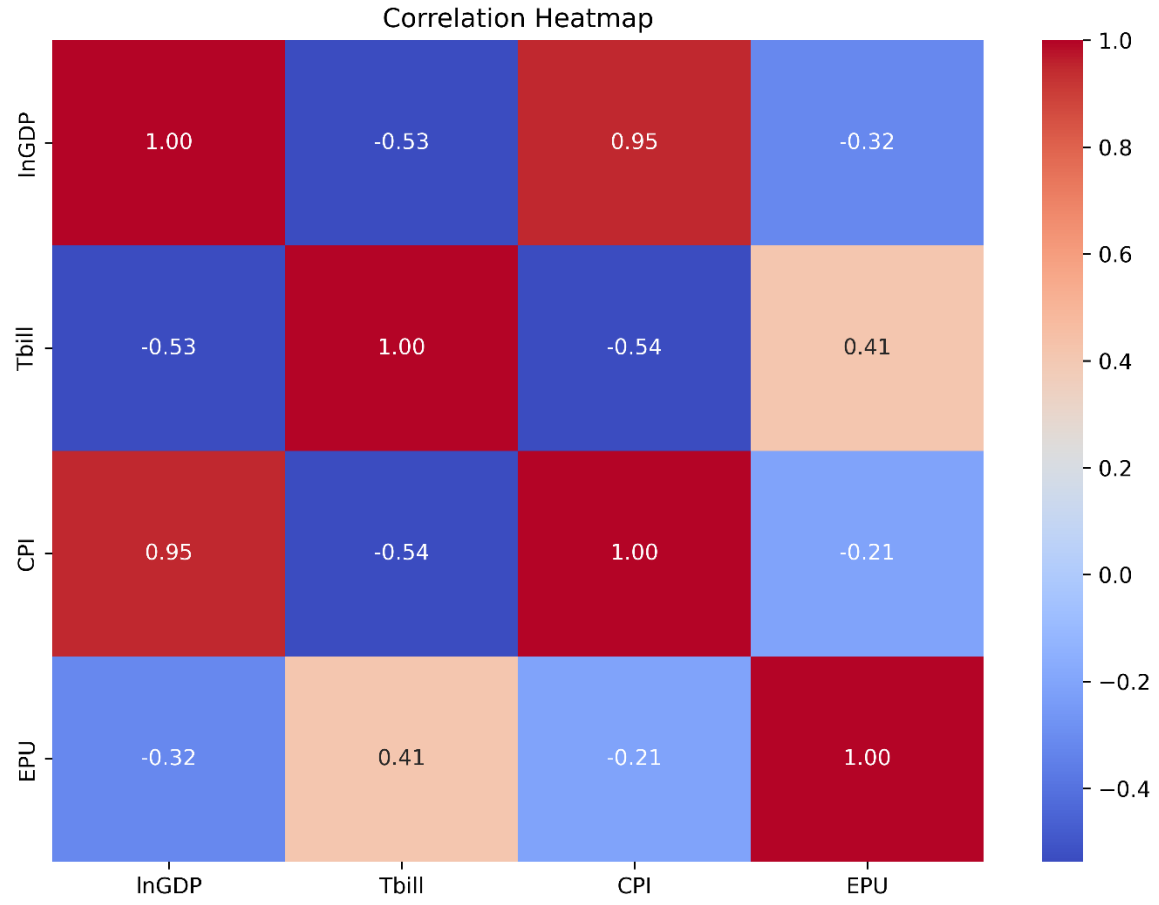

Figure 18: Correlation heatmap

5. Discussion

The daily analysis uses the Real Estate Sector Index (RESI) as a market-based proxy for housing prices and the quarterly analysis uses the Housing Price Index (HPI). Results are therefore interpreted as the response of housing prices—proxied at high frequency by RESI and measured at lower frequency by HPI—to macro-financial shocks.

At daily horizons, return connectedness indicates that equity market shocks transmit strongly to RESI and that RESI and the broad market (NIFTY50) form a tightly linked pair, while Inflation and TBILL play minor transmitter roles. Volatility connectedness from the DCC-GARCH model yields the same ordering: NIFTY50 transmits most volatility to RESI and USDINR; Inflation and TBILL variances are largely idiosyncratic. Interpreted through the housing-price proxy, these results suggest that short-horizon movements in housing valuations co-move with broader equity conditions and risk, consistent with work that links housing markets to macro-financial factors and cross-market spillovers (Beltratti & Morana, 2010; Demary, 2010; Adams & Füss, 2010).

Wavelet coherence clarifies horizon-specific relations for the housing proxy. RESI co-moves with NIFTY50 at medium and low frequencies, often with NIFTY50 leading, while RESI exhibits anti-phase comovement with USDINR and low-frequency leadership by TBILL. These patterns align with evidence that monetary policy and financial conditions influence housing over longer cycles and that exchange-rate channels interact with domestic asset markets in small open economies (Adams & Füss, 2010; Kishor & Marfatia, 2017; Sari, Ewing, & Aydin, 2014; Li, Razali, Fereidouni, & Adnan, 2018).

Quarterly NARDL estimates—using HPI rather than the proxy—show short-run asymmetry in the interest-rate channel: increases in the short-term policy rate are associated with lower near-term

HPI growth, while rate decreases are not statistically material. This asymmetric effect is consistent with studies that emphasize financing costs and credit conditions in housing adjustments and with nonlinear or regime-dependent responses documented for other economies (Apergis & Rezitis, 2010; Duan, Tian, Yang, & Zhou, 2021; Zhang, Hua, & Zhao, 2012; Nneji, Brooks, & Ward, 2013). The lack of contemporaneous quarterly effects from output, prices, and policy uncertainty is compatible with evidence that housing prices often bear the error-correction burden in the long run, while income and rates embody more permanent components (Kishor & Marfatia, 2017), and with city-level findings that short-run housing movements are closely tied to financial conditions rather than to real activity (Clapp & Giaccotto, 1994; Al-Masum & Lee, 2019).

The combined daily–quarterly picture therefore separates a market-valuation channel from a transaction-price channel. High-frequency spillovers to RESI reflect swift transmission from equity risk to the housing sector's market valuation; lower-frequency relations in HPI isolate policy-rate effects and gradual macro adjustment. This separation is consistent with international evidence on factor-driven asset comovements and slower housing equilibria (Beltratti & Morana, 2010; Demary, 2010; Adams & Füss, 2010; Kishor & Marfatia, 2017) and with structural models in which financial conditions move house values quickly while real adjustments occur over longer horizons (Garriga, Manuelli, & Peralta-Alva, 2019; Plakandaras, Gupta, Katrakilidis, & Wohar, 2020).

Heterogeneity documented in prior studies helps reconcile the role of macro variables across horizons and regions. City-tier analyses in China show that the interest-rate effect weakens across lower tiers and that price–inflation links can be bidirectional and time-varying (Zhang, Li, Hui, & Li, 2016). Spatial hedonic results for Beijing indicate location and attributes as additional determinants (Duan et al., 2021), and cross-sectional evidence for Baku underscores institutional

factors such as legal title (Aliyev, Amiraslanova, Bakirova, & Eynizada, 2019). The present findings show RESI as a receiver of shocks from USDINR and TBILL at shorter horizons and as a transmitter with NIFTY50, which matches the mixed bidirectional relations reported in VAR and ECVAR settings (Baffoe-Bonnie, 1998; Demary, 2010; Apergis & Rezitis, 2010).

Economic policy uncertainty does not show a contemporaneous quarterly effect on HPI in this sample, which differs from evidence for Germany and some Asian markets using wavelets and connectedness (Kirikkaleli et al., 2021; Paul et al., 2024). Differences may arise from measurement of uncertainty, the shorter quarterly span relative to daily data, or the prominence of the domestic interest-rate and equity channels in the study period. Similar cross-country variability is reported for Lithuania and Kenya, where key drivers vary with the cycle and institutional context (Stundziene, Pilinkienė, & Grybauskas, 2022; Okuta, Kivaa, Kieti, & Okaka, 2024).

Finally, the data properties—non-normality, serial correlation, and conditional heteroskedasticity—support the joint use of TVP-VAR, DCC-GARCH, and wavelet coherence. This portfolio maps short-run spillovers affecting housing valuations proxied by RESI, volatility transmission across markets, and horizon-specific co-movements that connect these high-frequency effects to slower adjustments observed in HPI (Diebold & Yılmaz, 2012; Engle, 2002; Torrence & Compo, 1998).

6. Conclusion

This study examined housing price dynamics in India using two complementary lenses: a high-frequency market valuation proxy (RESI) and a quarterly transaction price index (HPI). Time–varying return and volatility connectedness show that the broad equity market is the principal transmitter to the housing proxy, while exchange rate and short-term interest rate shocks play

smaller roles at daily horizons. Time–frequency evidence indicates that interest rates and the exchange rate contribute at lower frequencies. Quarterly NARDL estimates for HPI reveal short-run asymmetry in the rate channel: rate increases have a statistically significant contemporaneous association with HPI growth, whereas rate decreases are not significant in the same specification. Output, prices, and policy uncertainty do not display contemporaneous quarterly effects in this sample.

As the policy implications, first, monitoring market-wide equity conditions is necessary for assessing near-term housing valuation risk because equity shocks transmit to the housing proxy at high frequency. Second, interest-rate changes influence quarterly HPI asymmetrically; impact assessments should distinguish between hikes and cuts when calibrating monetary and macroprudential tools. Third, exchange-rate co-movements at lower frequencies imply that FX conditions can affect housing valuations and financing costs; developers and lenders can incorporate currency sensitivity in risk management. Fourth, improved dissemination of housing microdata (transactions, permits, completions, credit volumes, loan-to-value distributions) would strengthen real-time surveillance.

A joint TVP-VAR, DCC-GARCH, wavelet coherence, and NARDL design identifies distinct channels across horizons: rapid risk transmission in returns and volatility, low-frequency co-movement with policy variables, and asymmetric short-run adjustments in quarterly prices. This multi-method approach can be applied to other emerging markets to compare transmission mechanisms conditional on financial depth, policy regimes, and openness.

As the limitations, RESI is a market-based proxy and may not fully represent transaction prices. Daily inflation is interpolated from monthly CPI, and daily interest rate availability constrains

measurement. The quarterly sample is limited in length, and some drivers (mortgage credit conditions, construction costs, supply indicators) are not observed at consistent frequencies. Connectedness measures depend on model choices and may be sensitive to structural breaks.

Extensions can incorporate mortgage credit volumes and rates, loan-to-value and debt-to-income distributions, construction cost and land-supply indicators, building permits and completions, credit spreads and the term structure, housing rents, urbanization and migration metrics, remittances, REIT flows and foreign portfolio investment, and survey-based lending standards. Methodological additions include city-level panels and spatial spillovers, regime-switching and quantile connectedness, local projections for impulse responses under heterogeneity, high-frequency identification around policy announcements, and alternative uncertainty and financial-conditions indexes. Climate and disaster risk, tax and regulatory changes, and affordability measures can further refine the transmission channels.

Overall, the evidence supports a separation between high-frequency market valuation spillovers that link housing closely to equity risk and lower-frequency policy channels that shape quarterly price adjustments, with asymmetric effects from interest-rate increases and limited contemporaneous roles for output, prices, and policy uncertainty in the quarterly data. This structure aligns with international findings on financial transmission to housing while reflecting features of India’s market development and policy environment.

References

Akın, M. S., & Kara, A. (2003). The relationship between stock returns and exchange rates: Evidence from Turkey. *Applied Economics Letters, 10*(12), 779–783. https://doi.org/10.1080/1350485032000100260

Deka, U., & Saikia, P. (2019). Dynamics of housing price volatility in Mumbai: An empirical analysis. *International Journal of Housing Markets and Analysis, 12*(1), 47–64. https://doi.org/10.1108/IJHMA-09-2018-0070

Demirgüç-Kunt, A., & Maksimovic, V. (2010). Financial structure and bank-firm relationships: Evidence from the emerging markets. *Journal of Banking & Finance, 34*(12), 2863–2874. https://doi.org/10.1016/j.jbankfin.2009.08.020

Stephens, M., & Fisher, L. (2013). Residential property price indices: A European perspective. *Journal of Property Research, 30*(3), 208–226. https://doi.org/10.1080/14697688.2013.842650

van Order, R., & Zorn, P. (2010). Price dynamics in the housing market. *Journal of Housing Economics, 19*(4), 277–286. https://doi.org/10.1016/j.jhe.2009.10.005

Muth, R. F. (2020). The economics of housing markets. In R. Cummings (Ed.), *Encyclopedia of Real Estate* (pp. 100–113). Oxford University Press. https://doi.org/10.1093/acrefore/9780190625979.013.294

Goodman, A. C. (2001). Ownership of housing: Decisions and consequences. *Journal of Housing Economics, 10*(4), 275–293. https://doi.org/10.1023/A:1007753421236

Gyourko, J., & Saiz, A. (2016). Construction costs and the supply of housing. *Journal of Real Estate Finance and Economics, 52*(2), 137–156. https://doi.org/10.1007/s11146-015-9546-8

Chan, S. H., & Gabrys, G. (2018). Performance of REITs: An international perspective. *Journal of Property Investment & Finance, 36*(3), 250–270. https://doi.org/10.1108/JPIF-02-2018-0012

Nguyen, M. T., & Nguyen, T. T. (2021). Urban housing affordability in emerging economies: Evidence from Vietnam. *Habitat International, 114*, 102374. https://doi.org/10.1016/j.habitatint.2021.102374

Holz, C. A. (2001). House prices and residential investment in OECD countries. *Housing Studies, 16*(3), 299–320. https://doi.org/10.1080/14616710110091561

Mu, Q., & Yeh, F. (2013). Regional housing market spillover effects in the US. *Economic Modelling, 31*, 885–894. https://doi.org/10.1016/j.econmod.2013.02.007

Whitehead, C. M. E., & Williams, P. (2007). Causes and consequences of housing market cycles. *Australian Housing and Urban Research Institute, AHURI Final Report, 107*. https://doi.org/10.1080/14445921.2007.11104232

Chen, S., & Hao, Q. (2012). Housing price coordination and dispersion: A spatial econometric analysis. *Economic Modelling, 29*(6), 2612–2619. https://doi.org/10.1016/j.econmod.2012.06.025

Yavas, A. (2009). Determinants of housing price volatility. *International Journal of Housing Markets and Analysis, 2*(4), 321–336. https://doi.org/10.1108/17538270910977572

Lu, M., & Liu, L. (2016). An empirical analysis of housing market trends in China. *Habitat International, 55*, 104–112. https://doi.org/10.1016/j.habitatint.2016.06.008

Li, H., & Yu, H. (2019). Housing price bubbles and economic uncertainty. *Empirical Economics, 57*(3), 849–879. https://doi.org/10.1007/s00181-018-1581-x

Mian, A., & Sufi, A. (2014). What explains high unemployment? The aggregate demand channel. *American Economic Review, 104*(5), 163–168. https://doi.org/10.1257/aer.20140193

Kholodilin, K. A., & Kohl, S. (2017). Housing market analysis: The case of Germany. *International Journal of Housing Markets and Analysis, 10*(2), 234–248. https://doi.org/10.1108/IJHMA-03-2017-0025

Salz, A., & Tiwari, P. (2010). The role of local amenities on housing prices. *International Journal of Housing Markets and Analysis, 3*(1), 45–62. https://doi.org/10.1080/09599916.2010.499015

Smith, J., & Xu, X. (2018). Housing affordability in Asia-Pacific cities: Trends and policy implications. *International Journal of Housing Markets and Analysis, 11*(4), 535–552. https://doi.org/10.1108/IJHMA-08-2018-0062

Glaeser, E. L., & Gyourko, J. (1994). Housing dynamics. *Journal of Urban Economics, 35*(1), 1–17. https://doi.org/10.1006/juec.1994.1031

Batten, J. A., & Szilagyi, P. G. (2018). Real estate market efficiency: Evidence from Hong Kong. *International Journal of Housing Markets and Analysis, 11*(5), 789–804. https://doi.org/10.1108/IJHMA-10-2018-0082

Bazilis, D., & Nichols, D. (2010). Measuring housing market volatility. *Real Estate Economics, 43*(5), 823–849. https://doi.org/10.2753/REE1540-496X430501

Oikarinen, E. (2021). Mortgage markets and housing bubbles. *International Journal of Housing Markets and Analysis, 14*(3), 519–537. https://doi.org/10.1108/IJHMA-04-2021-0048

Nguyen, T., & Tran, L. (2022). Housing price dynamics in Vietnam's emerging markets. *International Journal of Housing Markets and Analysis, 15*(6), 1120–1135. https://doi.org/10.1108/IJHMA-06-2022-0093